Forum of Mathematics, Sigma (2023), **Vol. 11**:e105 1–25
doi:10.1017/fms.2023.106

CAMBRIDGE UNIVERSITY PRESS

RESEARCH ARTICLE

t-Design Curves and Mobile Sampling on the Sphere

Martin Ehler[1] and Karlheinz Gröchenig[2]

[1]University of Vienna, Faculty of Mathematics, Oskar-Morgenstern-Platz 1, A-1090 Wien, Austria;
E-mail: martin.ehler@univie.ac.at.
[2]University of Vienna, Faculty of Mathematics, Oskar-Morgenstern-Platz 1, A-1090 Wien, Austria;
E-mail: karlheinz.groechenig@univie.ac.at.

Received: 12 June 2023; **Revised:** 29 August 2023; **Accepted:** 15 October 2023

2020 Mathematics Subject Classification: *Primary* – 41A55; *Secondary* – 41A63, 94A12, 26B15

Abstract

In analogy to classical spherical t-design points, we introduce the concept of t-design curves on the sphere. This means that the line integral along a t-design curve integrates polynomials of degree t exactly. For low degrees, we construct explicit examples. We also derive lower asymptotic bounds on the lengths of t-design curves. Our main results prove the existence of asymptotically optimal t-design curves in the Euclidean 2-sphere and the existence of t-design curves in the d-sphere.

Contents

1. Introduction

Spherical designs are point sets in the sphere $\mathbb{S}^d = \{x \in \mathbb{R}^{d+1} : \|x\| = 1\}$ that yield exact quadrature rules with constant weights for polynomial spaces. Thus, a finite set $X_t \subseteq \mathbb{S}^d$ is a t-design (or X_t consists of t-design points) if for every algebraic polynomial f in $d+1$ variables of (total) degree t, one has

$$\frac{1}{|X_t|}\sum_{x\in X_t} f(x) = \int_{\mathbb{S}^d} f\,. \tag{1}$$

This concept plays an important role in numerical analysis, approximation theory and many related fields, and the theory, construction and applications of spherical designs has become a highly developed art. See [10, 40, 41] and [5, 21, 42, 48] for a sample of papers on spherical t-design points. In particular, the existence of asymptotically optimal t-design points in the d-sphere has long been an open problem and has eventually been proved by Bondarenko, Radchenko and Viazovska in [3].

In this paper, we study a variation where points are replaced by curves. The goal is again to obtain quadrature formulas along curves in the sphere that are exact for polynomials of a given degree. The central notion is the definition of a t-design curve. Precisely, a closed, piecewise smooth curve $\gamma : [0,1] \to \mathbb{S}^d$ with at most finitely many self intersections and with arc length $\ell(\gamma)$ is called a t-design curve in $\mathbb{S}^d$ if the line integral integrates exactly all algebraic polynomials in $d+1$ variables of degree t,

$$\frac{1}{\ell(\gamma)}\int_\gamma f = \int_{\mathbb{S}^d} f\,. \tag{2}$$

The use of curves instead of point evaluations in definition (2) is motivated by numerous analogous applications of curves for the collection and processing of data on the sphere. Here is a short list of applications of curves in a similar spirit: Low-discrepancy curves were discussed in [35] as an efficient coverage of space with applications in robotics. See also the textbook [30] on robotics, where curves are derived for motion planning to obtain an optimal path under several side constraints. Space-filling curves are used as dimensionality reduction tools in optimization, image processing and deep learning cf. [20, 8, 44]. Curves are applied in [14] to approximate probability measures. The concept of principal curves is discussed in [24, 23, 28, 31] to best fit given data. In another statistical context, the information tuning curve quantifies discriminatory abilities of populations of neurons [37, 27]. Motivated by more geometric questions, length and thickness of ropes on spheres are studied in [17, 18] as variants of packing problems. In the context of optimization problems, the shortest closed space curve to inspect a sphere is determined in [19]; variations are discussed in [50]. Energy minimization and geometric arrangements in biophysics lead to optimality questions of knots and ropes [7, 33, 49]. In mobile sampling, curve trajectories provide sampling sets that enable efficient signal reconstruction [2, 25, 22, 26, 46, 45, 36].

Our goal is to study integration on the sphere by using information along closed curves rather than point evaluations. The new notion of t-design curves in (2) addresses exact integration on the sphere along curves and the related problem of the exact reconstruction of bandlimited functions on the sphere. The pertinent questions of t-design curves on spheres are similar to those of spherical t-design points.

Problem (A): What is the minimal (order of the) arc length of a t-design curve?

Problem (B): Do t-design curves exist on $\mathbb{S}^d$ for all $t \in \mathbb{N}$?

Problem (C): If yes, are there t-design curves on $\mathbb{S}^d$ achieving the optimal order of arc length?

Problem (D): Provide explicit constructions of t-design curves.

The answers to the analogous questions for t-design points have a long history and culminate in the solution of the Korevaar-Meyers conjecture by Bondarenko, Radchenko and Viazovska [3] mentioned above.

Our program is to make a first attempt at these questions for t-design *curves* on d-spheres. We will offer answers to (A) and (B) and give a solution of problem (C) on the sphere $\mathbb{S}^2$. As a contribution to Problem (D), we will construct some examples of smooth t-design curves for small degrees t.

Results. In the following, we denote the space of algebraic polynomials of $d+1$ real variables of (total) degree t by Π_t. As a necessary condition for the length of a t-design curve, we obtain the following answer to Problem (A).

https://doi.org/10.1017/fms.2023.106 Published online by Cambridge University Press

Theorem 1.1. *Assume that a piecewise smooth, closed curve* $\gamma : [0,1] \to \mathbb{S}^d$ *satisfies*

$$\frac{1}{\ell(\gamma)} \int_\gamma f = \int_{\mathbb{S}^d} f \qquad \text{for all } f \in \Pi_t .$$

Then its length is bounded from below by

$$\ell(\gamma) \geq C_d t^{d-1}$$

with some constant $C_d > 0$ *that may depend on the dimension* d *but is independent of* t *and* γ.

By comparison, a spherical t-design requires $|X_t| \asymp t^d$ points [9, 40, 10].[1]

The next challenge is to prove the existence of t-design curves that match the asymptotic order t^{d-1}. For the unit sphere in $\mathbb{R}^3$, we succeeded in proving the existence. This solves Problem (C) for $\mathbb{S}^2$.

Theorem 1.2. *In* $\mathbb{S}^2$ *there exists a sequence of* t*-design curves* $(\gamma_t)_{t\in\mathbb{N}}$ *with length* $\ell(\gamma_t) \asymp t$.

Note that even for $d = 2$, the corresponding problem of the existence of spherical t-designs points was solved only in 2011 [3]. In our proof, we will make substantial use of the result from [3]. In dimension $d \geq 3$, we prove the existence of t-design curves. This is a solution to Problem (B).

Theorem 1.3. *In* $\mathbb{S}^d$ *for* $d \geq 3$*, there exists a sequence of* t*-design curves* $(\gamma_t)_{t\in\mathbb{N}}$*, such that* $\ell(\gamma_t) \lesssim t^{d(d-1)/2}$.

This asymptotic order does not match our lower bounds for $d \geq 3$ in Theorem 1.1. In the analogous problem of t-design points, our Theorem 1.3 corresponds to the upper bounds of Korevaar and Meyers [29] from 1993. It remains an interesting challenge to derive the existence of t-design curves on $\mathbb{S}^d$ that match the bounds of Theorem 1.1.

The existence theorems are constructive only in part, as they are based on the non-constructive results of Bondarenko, Radchenko and Viazovska [3]. We will describe a procedure that associates to every set of t-design points in $\mathbb{S}^d$ a corresponding t-design curve. This part is constructive, and the result is a closed, piecewise smooth curve that consists of arcs of Euclidean circles (by a circle in $\mathbb{S}^d$, we mean a circle in the intersection of a 2-dimensional subspace of $\mathbb{R}^{d+1}$ with $\mathbb{S}^d$).

As a small contribution to Problem (D), we will discuss some explicit constructions of smooth t-design curves for very low polynomial degrees ($t = 1, 2, 3$). Explicit constructions of t-design points and curves remain a difficult problem with many open threads.

Mobile sampling. Mobile sampling refers to the approximation or reconstruction of a function from its values along a curve [45, 46]. The rationale for this mode of data acquisition is the small number of required sensors. Sampling a function along a curve requires only one sensor, whereas the sampling at a point set (e.g., t-design points) requires many sensors. In engineering applications, it is natural to assume that the function f to be sampled is bandlimited on $\mathbb{R}^d$ (i.e., the support of the Fourier transform $\hat{f}$ is compact).

Transferred to the sphere $\mathbb{S}^d$, a function on the sphere is bandlimited if it is a polynomial restricted to the sphere. Its degree is a measure for the bandwidth. A typical and natural scenario for mobile sampling on the sphere would be the surveillance of meteorological or geophysical data along airplane routes. The goal would be to reconstruct the complete data globally, which means literally on the entire 'globe' (i.e., $\mathbb{S}^2$). The connection between t-design curves and mobile sampling on the sphere is explained in the following statement.

Corollary 1.4. *Let* γ *be a* $2t$*-design curve on* $\mathbb{S}^d$ *and* f *a polynomial of degree* t*. Then*

$$\frac{1}{\ell(\gamma)} \int_\gamma |f|^2 = \int_{\mathbb{S}^d} |f|^2 . \tag{3}$$

Furthermore, f *is uniquely determined by its values along* γ.

[1] We write $\lesssim$ if the left-hand side is bounded by a constant times the right-hand side. If $\lesssim$ and $\gtrsim$ both hold, then we write $\asymp$.

https://doi.org/10.1017/fms.2023.106 Published online by Cambridge University Press

Clearly, (3) follows immediately from the assumption because $f \in \Pi_t$ implies that $|f|^2 \in \Pi_{2t}$. The uniqueness and an explicit reconstruction formula will be derived in Section 7.

We also discuss some elementary consequences of t-design curves on the sphere in high-dimensional Euclidean quadrature. Generalized Gauss-Laguerre quadrature combined with spherical t-design curves lead to exact integration of polynomials of total degree t with respect to the measure $e^{-\|x\|}dx$ on $\mathbb{R}^d$.

Methods. Both Theorems 1.1 and 1.2 are based on the existence of optimal t-design points. An immediate guess would be to connect t-design points along geodesic arcs in $\mathbb{S}^d$ and hope that a suitable order of points would yield a t-design curve. As there are $O(t^d)$ points in a t-design with a distance $O(t^{-1})$ to the nearest neighbor, the solution of the traveling salesman problem would lead to a curve of the desired length $O(t^{d-1})$ [14, Lemma 3]. However, so far this idea has not been fruitful, and we do not know how such a path would yield exact quadrature.

Our idea is to connect the point evaluation $f \to f(x), x \in \mathbb{S}^d$ to an integral over the boundary of a spherical cap by means of a formula of Samko [39]. In $\mathbb{S}^2$, the boundary of a spherical cap is a circle, and thus the union of such circles with centers at t-design points yields a first quadrature rule. To generate a single closed curve from this union of circles, we invoke some combinatorial arguments from graph theory, such as spanning trees and Eulerian paths. The extension to higher dimensions is by induction on the dimension d. Here we need some additional properties from spherical geometry.

Outlook. Spherical t-design points have proved a rich field of research with deep mathematical questions. The new theory of t-design curves offers a similarly rich playground for both challenging mathematics and for the investigation of associated numerical and computational questions and applications.

On the mathematical side, the most immediate question is the existence of t-design curves of asymptotically optimal length in $\mathbb{S}^d$ for $d \geq 3$. Another direction is the exploration of t-design curves on general compact Riemannian manifolds (extending the work on t-design points in [13, 15, 16]). Theorem 1.1 on the lower bound on the length of a t-design curve carries over to the manifold setting, but all constructive aspects are wide open.

Next, one might want to impose additional conditions on the curves. Our construction yields piecewise smooth, closed curves with finitely many corners and self-intersections. For aesthetical reasons, one might want t-design curves to be smooth and simple (i.e., without corners and self-intersections). So far, we know such examples only for degrees $t \leq 3$ on $\mathbb{S}^2$. Other aspects to be considered might be curvature, contractibility (or other homotopy constraints) or the ratio between inner and outer area for closed curves on surfaces. At this time, we are far from understanding any of these questions.

The outline is as follows: In Section 2, we introduce the concept of t-design curves in $\mathbb{S}^d$, and we derive asymptotic lower bounds on the curves' length. Smooth spherical t-design curves in $\mathbb{S}^2$ for $t = 1, 2, 3$ are provided in Section 3. Section 4 is dedicated to some preparations for our two main theorems. The first one on the existence of asymptotically optimal t-design curves in $\mathbb{S}^2$ is derived in Section 5. The existence of t-design curves in $\mathbb{S}^d$ is proved in Section 6. In Section 7, we briefly discuss the use of t-design curves in mobile sampling and for high-dimensional quadrature on $\mathbb{R}^d$.

2. From points to curves

We denote the collection of classical polynomials of total degree at most $t \in \mathbb{N}$ in $d+1$ variables on $\mathbb{R}^{d+1}$ by Π_t. Each $f \in \Pi_t$ can be evaluated on the unit sphere $\mathbb{S}^d = \{x \in \mathbb{R}^{d+1} : \|x\| = 1\}$. We always use the normalized surface measure, so that $\int_{\mathbb{S}^d} 1 = 1$. The (rotation-) invariant metric on $\mathbb{S}^d$ is

$$\operatorname{dist}(x, y) = \arccos\langle x, y\rangle \,. \tag{4}$$

It measures the length of the geodesic arc connecting x and y on $\mathbb{S}^d$.

https://doi.org/10.1017/fms.2023.106 Published online by Cambridge University Press

2.1. t-design points

For $t \in \mathbb{N}$, a finite set $X \subset \mathbb{S}^d$ is called *t-design points* (or simply t-design) in $\mathbb{S}^d$ if

$$\frac{1}{|X|} \sum_{x \in X} f(x) = \int_{\mathbb{S}^d} f, \qquad \forall f \in \Pi_t. \tag{5}$$

We call $(X_t)_{t \in \mathbb{N}}$ a *sequence of t-design points* in $\mathbb{S}^d$ if each X_t is a t-design for $t \in \mathbb{N}$.

It turns out that each sequence $(X_t)_{t \in \mathbb{N}}$ of t-design points in $\mathbb{S}^d$ must satisfy

$$|X_t| \gtrsim t^d, \qquad t \in \mathbb{N}, \tag{6}$$

where the constant may depend on d but is independent of t, cf. [6]. A sequence of t-design points $(X_t)_{t \in \mathbb{N}}$ in $\mathbb{S}^d$ is called *asymptotically optimal* if

$$|X_t| \asymp t^d, \qquad t \in \mathbb{N}.$$

Again, we allow the constant to depend on d. Asymptotically optimal point sequences do exist [3, 13, 15, 16].

2.2. t-design curves

We now introduce a new concept by switching from points to a curve. By a curve, we mean a continuous, piecewise differentiable function $\gamma : [0, 1] \to \mathbb{S}^d$ with at most finitely many self-intersections. Since the sphere is a closed manifold, we only consider closed curves.

We may interpret γ as a space curve in $\mathbb{R}^{d+1}$, so that its length is

$$\ell(\gamma) = \int_0^1 \|\dot\gamma(s)\| \mathrm{d}s,$$

where the speed $\|\dot\gamma\|$ of the curve is defined almost everywhere. The line integral is

$$\int_\gamma f = \int_0^1 f(\gamma(s)) \|\dot\gamma(s)\| \mathrm{d}s,$$

so that $\ell(\gamma) = \int_\gamma 1$. Note that $\int_\gamma f$ does not depend on the parametrization and orientation of the curve.

In analogy to (5), we now introduce t-design curves.

Definition 2.1. For $t \in \mathbb{N}$, we say that γ is a *t-design curve* in $\mathbb{S}^d$ if

$$\frac{1}{\ell(\gamma)} \int_\gamma f = \int_{\mathbb{S}^d} f, \qquad f \in \Pi_t. \tag{7}$$

A sequence of curves $(\gamma_t)_{t \in \mathbb{N}}$ is called a sequence of *t-design curves* in $\mathbb{S}^d$ if each γ_t is a t-design for $t \in \mathbb{N}$.

Analogously to (6), one now expects lower asymptotic bounds on $\ell(\gamma_t)$; see also [14, Theorem 3 in Section 5]. The following is Theorem 1.1 of the Introduction.

Theorem 2.2. *If $(\gamma_t)_{t \in \mathbb{N}}$ a sequence of t-design curves in $\mathbb{S}^d$, then*

$$\ell(\gamma_t) \gtrsim t^{d-1}, \quad t \in \mathbb{N}. \tag{8}$$

https://doi.org/10.1017/fms.2023.106 Published online by Cambridge University Press

Proof. We use some results from [6] and [4]. Let $\Gamma_t = \gamma_t([0,1])$ be the trajectory of γ_t. The covering radius ρ_t of Γ_t is defined as

$$\rho_t := \sup_{x\in\mathbb{S}^d}\left(\inf_{y\in\Gamma_t} \operatorname{dist}(x,y)\right). \tag{9}$$

By this definition, there is $x \in \mathbb{S}^d$ such that the closed ball $B_{\rho_t/2}(x) = \{y \in \mathbb{S}^d : \operatorname{dist}(x,y) \le \frac{\rho_t}{2}\}$ of radius $\rho_t/2$ centered at x does not intersect Γ_t; that is,

$$B_{\rho_t/2}(x) \cap \Gamma_t = \emptyset. \tag{10}$$

Let us denote the Laplace-Beltrami operator on the sphere $\mathbb{S}^d$ by Δ and the identity operator by I. According to [6, Lemma 5.2 with $s = 2d$ and $p = 1$], see also [4] for the original idea, there is a function f_t supported on $B_{\rho_t/2}(x)$ such that

$$\|(I-\Delta)^d f_t\|_{L^1(\mathbb{S}^d)} \lesssim 1, \qquad \text{and} \qquad \rho_t^{2d} \lesssim \int_{\mathbb{S}^d} f_t. \tag{11}$$

Since (10) implies $\int_{\gamma_t} f_t = 0$, the t-design assumption and [4, Theorem 2.12] lead to

$$\left|\int_{\mathbb{S}^d} f_t\right| \lesssim t^{-2d}\|(I-\Delta)^d f_t\|_{L^1}. \tag{12}$$

By combining (12) with (11), we deduce $\rho_t^{2d} \lesssim t^{-2d}$, so that

$$\rho_t \lesssim t^{-1}. \tag{13}$$

To relate ρ_t with $\ell(\gamma_t)$, we apply a packing argument. Let n be the maximum number of disjoint balls of radius $2\rho_t$ in $\mathbb{S}^d$ (i.e., $B_{2\rho_t}(x_j) \cap B_{2\rho_t}(x_k) = \emptyset$ for $j,k = 1,\dots,n$ with $j \neq k$). Then the balls $B_{4\rho_t}(x_j)$ cover $\mathbb{S}^d$; otherwise, there is $x \in \mathbb{S}^d$, such that $x \notin \bigcup_{j=1}^n B_{4\rho_t}(x_j)$ and $B_{2\rho_t}(x)$ is disjoint from all $B_{2\rho_t}(x_j)$, contradicting the maximality of n.

We note that every ball $B_r(x)$ in $\mathbb{S}^d$ with radius $0 < r \le 1$ has volume $\operatorname{vol}(B_r(x)) \asymp r^d$. Consequently,

$$1 \le \sum_{j=1}^n \operatorname{vol}(B_{4\rho_t}(x_j)) \lesssim n\rho_t^d,$$

so that we obtain

$$n \gtrsim \rho_t^{-d}.$$

This is known as the Gilbert-Varshamov bound in coding theory, cf. [1].

Since $B_{2\rho_t}(x_j) \cap B_{2\rho_t}(x_k) = \emptyset$, the distance between two distinct balls $B_{\rho_t}(x_j)$ and $B_{\rho_t}(x_k)$ is at least $2\rho_t$. Due to the definition of the covering radius ρ_t and the compactness of Γ_t and $\mathbb{S}^d$, the trajectory Γ_t intersects each ball $B_{\rho_t}(x_k)$. Therefore, the length of γ_t must satisfy

$$\ell(\gamma_t) \gtrsim n\rho_t \gtrsim \rho_t^{1-d}. \tag{14}$$

Since (13) is equivalent to $\rho_t^{-1} \gtrsim t$, the bound (14) leads to

$$\ell(\gamma_t) \gtrsim \rho_t^{1-d} \gtrsim t^{d-1}. \qquad \square$$

The lower bound on the length of γ_t leads to the concept of asymptotic optimality for curves.

https://doi.org/10.1017/fms.2023.106 Published online by Cambridge University Press

Definition 2.3. A sequence $(\gamma_t)_{t\in\mathbb{N}}$ of t-design curves in $\mathbb{S}^d$ is called *asymptotically optimal* if

$$\ell(\gamma_t) \asymp t^{d-1}, \qquad t \in \mathbb{N}.$$

In the remainder of the paper, we study the existence of t-design curves on the sphere $\mathbb{S}^d$.

3. Some spherical t-design curves for small t in $\mathbb{S}^2$

Here we construct smooth t-design curves in $\mathbb{S}^2$ for $t = 1, 2, 3$. For $1 \le k \in \mathbb{N}$ and $a \in [0, 1]$, consider the family of curves $\gamma^{(k,a)} : [0, 1] \to \mathbb{S}^2$ given by

$$\gamma^{(k,a)}(s) := \begin{pmatrix} a\cos(2\pi s) + (1-a)\cos(2\pi(2k-1)s) \\ a\sin(2\pi s) - (1-a)\sin(2\pi(2k-1)s) \\ 2\sqrt{a(1-a)}\sin(2\pi k s) \end{pmatrix}. \tag{15}$$

If $k = 1$, then $\gamma^{(k,a)}$ describes a great circle, and it is easy to see that every great circle in $\mathbb{S}^d$ yields a 1-design. The family $\gamma^{(k,a)}$ also gives rise to spherical 2-design and 3-design curves.

Proposition 3.1. *The curves $\gamma^{(k,a)}$ have the following properties:*

(i) *$\gamma^{(k,a)}$ is a 1-design curve for all $k \in \mathbb{N}$.*
(ii) *There is $a_2 \in (\frac{1}{2}, 1)$ such that $\gamma^{(2,a_2)}$ is a 2-design curve.*
(iii) *For $k \ge 3$, there is $a_k \in (\frac{1}{2}, 1)$ such that $\gamma^{(k,a_k)}$ is a 3-design curve.*

To verify Proposition 3.1, recall that the surface measure on $\mathbb{S}^2$ is normalized, so that $\int_{\mathbb{S}^2} 1 = 1$. Due to the sphere's symmetries, integrals over the sphere of every monomial of odd degree vanish. Moreover, when x, y, z denote the coordinate functions in $\mathbb{R}^3$, we have

$$0 = \int_{\mathbb{S}^2} xy = \int_{\mathbb{S}^2} xz = \int_{\mathbb{S}^2} yz, \tag{16}$$

$$\frac{1}{3} = \int_{\mathbb{S}^2} x^2 = \int_{\mathbb{S}^2} y^2 = \int_{\mathbb{S}^2} z^2. \tag{17}$$

By definition of length, we directly observe

$$\int_{\mathbb{S}^2} 1 = 1 = \frac{1}{\ell(\gamma^{(k,a)})} \int_0^1 \|\dot\gamma^{(k,a)}(s)\| \mathrm{d}s = \frac{1}{\ell(\gamma^{(k,a)})} \int_{\gamma^{(k,a)}} 1. \tag{18}$$

To treat line integrals of the other monomials, will use the following lemma.

Lemma 3.2. *There are real-valued coefficients $(c_n^{(k,a)})_{n\in\mathbb{N}} \in \ell^1(\mathbb{Z})$ such that*

$$\|\dot\gamma^{(k,a)}(s)\| = \sum_{n\in\mathbb{N}} c_n^{(k,a)} \cos(4\pi k n s),$$

and $\gamma^{(k,a)}$ has an arc length parametrization.

Proof of Lemma 3.2. The arc length parametrization exists whenever $\|\dot\gamma^{(k,a)}(s)\|$ is positive. Indeed, an elementary calculation reveals that

$$\|\dot\gamma^{(k,a)}(s)\|^2 = \alpha^{(k,a)} + \beta^{(k,a)}\cos(4\pi k s) \tag{19}$$

https://doi.org/10.1017/fms.2023.106 Published online by Cambridge University Press

with the nonnegative constants

$$\alpha^{(k,a)} = 4\pi^2\Big((2k-1)^2 - 2a(3k^2-4k+1) + 2a^2(k-1)^2\Big) \tag{20}$$

$$= 4\pi^2\Big(a^2 + (2k-1)^2(1-a)^2 + 2k^2a(1-a)\Big), \tag{21}$$

$$\beta^{(k,a)} = 8\pi^2 a(1-a)(k-1)^2. \tag{22}$$

Their difference

$$\alpha^{(k,a)} - \beta^{(k,a)} = 4\pi^2\Big(a^2 + (2k-1)^2(1-a)^2 + 2a(1-a)(2k-1)\Big) \tag{23}$$

is positive for all $a \in [0,1]$, so that also $\|\dot\gamma^{(k,a)}(s)\|^2$ is positive for all $s \in \mathbb{R}$. The theorem of Wiener Lévy implies that $s \mapsto \|\dot\gamma^{(k,a)}(s)\|$ possesses an absolutely convergent Fourier series. Since $\|\dot\gamma^{(k,a)}(s)\|^2$ has period $1/(2k)$, its square root has the same period, and thus only terms of the form $\cos(4\pi kns)$ appear in the Fourier series of $\|\dot\gamma^{(k,a)}(s)\|$. □

Proof of Proposition 3.1. (i) Exact integration of the constant function has already been checked in (18). Since $\gamma^{(k,a)}$ does not contain any term of the form $\cos(4\pi kns)$ for $n \in \mathbb{N}$, Lemma 3.2 and the orthogonality relations of the Fourier basis imply

$$\int_0^1 \gamma^{(k,a)}(s)\|\dot\gamma^{(k,a)}(s)\|\mathrm{d}s = 0,$$

which matches the requirement that integrals of degree 1 monomials vanish.

(ii) For $k \geq 2$, by the definition of $\gamma^{(k,a)}$, its x and y-coordinates are trigonometric polynomials of degree $\leq 2k-1$ and the z-coordinate is a trigonometric polynomial of degree k, consequently the product of two distinct components of $\gamma^{(k,a)}$ is a trigonometric polynomial of degree at most $4k-2$ without a constant term. Therefore, the products xy, xz, yz do not contain any term of the form $\cos(4\pi nkt)$, for $n \in \mathbb{N}$, and we deduce

$$0 = \int_{\gamma^{(k,a)}} xy = \int_{\gamma^{(k,a)}} xz = \int_{\gamma^{(k,a)}} yz,$$

which matches the identities (16) for the monomials of degree 2.

One sees directly from the definition of the coordinates of $\gamma^{(k,a)}$ that

$$\int_{\gamma^{(k,a)}} x^2 = \int_{\gamma^{(k,a)}} y^2.$$

Let $c_0^{(k,a)} = \ell(\gamma^{(k,a)})$ and $c_1^{(k,a)}$ be the coefficients in Lemma 3.2. We now need to investigate

$$\frac{1}{\ell(\gamma^{(k,a)})}\int_{\gamma^{(k,a)}} z^2 = 2a(1-a)\left(1 - \frac{\frac{1}{2}c_1^{(k,a)}}{c_0^{(k,a)}}\right) =: \eta(a)\,. \tag{24}$$

We aim for a parameter a_k such that (24) equals $\frac{1}{3}$, but we cannot solve this directly. For $a = 0$ and $a = 1$, the expression vanishes. We will verify that $\eta(1/2) > 1/3$. Then the continuity in a and the intermediate value theorem ensure that there is $a_k \in (\frac{1}{2}, 1)$ such that $\eta(a_k) = 1/3$.

https://doi.org/10.1017/fms.2023.106 Published online by Cambridge University Press

Rewriting (24) for $a = \frac{1}{2}$, we note that $\eta(\frac{1}{2}) \geq \frac{1}{3}$, if and only if

$$\frac{\frac{1}{2}c_1^{(k,\frac{1}{2})}}{c_0^{(k,\frac{1}{2})}} \leq \frac{1}{3}\,. \tag{25}$$

To obtain a lower bound on $c_0^{(k,\frac{1}{2})}$, we observe that by (23), $\alpha^{(k,\frac{1}{2})} - \beta^{(k,\frac{1}{2})} = 4\pi^2 k^2$. Therefore, we have

$$\sqrt{\alpha^{(k,\frac{1}{2})} + \beta^{(k,\frac{1}{2})}\cos(4\pi k s)} \geq \sqrt{\alpha^{(k,\frac{1}{2})} - \beta^{(k,\frac{1}{2})}} \geq 2\pi k,$$

which leads to

$$c_0^{(k,\frac{1}{2})} = \int_0^1 \sqrt{\alpha^{(k,\frac{1}{2})} + \beta^{(k,\frac{1}{2})}\cos(4\pi k s)}\mathrm{d}s \geq 2\pi k\,.$$

To obtain an upper bound on $\frac{1}{2}c_1^{(k,\frac{1}{2})}$, we first observe that the substitution $s' = 2ks$ and periodicity lead to

$$\begin{aligned}\frac{1}{2}c_1^{(k,\frac{1}{2})} &= \int_0^1 \sqrt{\alpha^{(k,\frac{1}{2})} + \beta^{(k,\frac{1}{2})}\cos(4\pi k s)}\cos(4\pi k s)\mathrm{d}s \\ &= \int_0^1 \sqrt{\alpha^{(k,\frac{1}{2})} + \beta^{(k,\frac{1}{2})}\cos(2\pi s)}\cos(2\pi s)\mathrm{d}s\,.\end{aligned}$$

We bound the positive part $\int_{-\frac{1}{4}}^{\frac{1}{4}} \ldots$ and the negative part $\int_{\frac{1}{4}}^{\frac{3}{4}} \ldots$ separately. The observation $\alpha^{(k,\frac{1}{2})} + \beta^{(k,\frac{1}{2})} = 4\pi^2(2k^2 - 2k + 1) \leq 8\pi^2 k^2$ leads to

$$\int_{-\frac{1}{4}}^{\frac{1}{4}} \sqrt{\alpha^{(k,\frac{1}{2})} + \beta^{(k,\frac{1}{2})}\cos(2\pi s)}\cos(2\pi s)\mathrm{d}s \leq \int_{-\frac{1}{4}}^{\frac{1}{4}} \sqrt{8}\pi k\cos(2\pi s)\mathrm{d}s = \sqrt{8}k\,.$$

For the negative part, we recall $\alpha^{(k,\frac{1}{2})} + \beta^{(k,\frac{1}{2})}\cos(2\pi s) \geq \alpha^{(k,\frac{1}{2})} - \beta^{(k,\frac{1}{2})} = 4\pi^2 k^2$ and obtain

$$\int_{\frac{1}{4}}^{\frac{3}{4}} \sqrt{\alpha^{(k,\frac{1}{2})} + \beta^{(k,\frac{1}{2})}\cos(2\pi s)}\cos(2\pi s)\mathrm{d}s \leq \int_{\frac{1}{4}}^{\frac{3}{4}} 2\pi k\cos(2\pi s)\mathrm{d}s = -2k\,.$$

Combining these bounds, we derive

$$\frac{1}{2}c_1^{(k,\frac{1}{2})} \leq (\sqrt{8} - 2)k \leq k.$$

Therefore, we do have

$$\frac{\frac{1}{2}c_1^{(k,\frac{1}{2})}}{c_0^{(k,\frac{1}{2})}} \leq \frac{1}{2\pi} < \frac{1}{3}\,.$$

The intermediate value theorem ensures that we can match (17).

(iii) The integrals over $\mathbb{S}^2$ of the monomials of degree 3 vanish. For $k \geq 3$, a product of 3 components of $\gamma^{(k,a)}$ does not contain any terms of the form $\cos(4\pi k n s)$, where $n \in \mathbb{N}$. Lemma 3.2 implies that the integral over $\gamma^{(k,a)}$ of every degree 3 monomial vanishes. □

https://doi.org/10.1017/fms.2023.106 Published online by Cambridge University Press

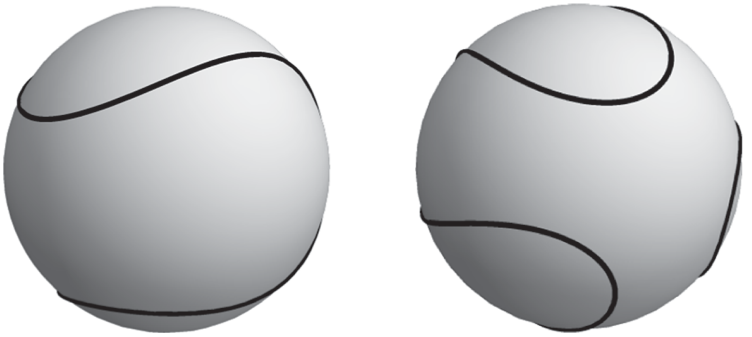

(a) $\gamma^{(2,a_2)}$ (b) $\gamma^{(3,a_3)}$

Figure 1. *Curves in Example 3.3: $\Gamma^{(2,a_2)}$ and $\gamma^{(3,a_3)}$ are smooth curves, and $\gamma^{(2,a_2)}$ resembles the seam of a tennis ball.*

Example 3.3. The values $a_2 \approx 0.7778$ and $a_3 \approx 0.7660$ lead to the trajectories $\Gamma^{(2,a_2)}$ and $\Gamma^{(3,a_3)}$ depicted in Figure 1. The lengths satisfy $\ell(\gamma^{(2,a_2)}) \approx 9.786$, and $\ell(\gamma^{(3,a_3)}) \approx 14.232$.

4. Preparatory results

We will derive two preparatory results that are needed for our main theorems in subsequent sections. The first one is about the connectivity of a graph associated to a covering, and the second one is about the integration along the boundary of spherical caps.

4.1. Connectivity of graphs associated to coverings

The spherical cap of radius $0 < r < \frac{\pi}{2}$ centered at $x \in \mathbb{S}^d$ is

$$B_r(x) = \{z \in \mathbb{S}^d : \operatorname{dist}(x, z) \leq r\}.$$

To every finite set $X \subseteq \mathbb{S}^d$ and $r > 0$, we associate a graph $\mathcal{G}_r$ as follows: its vertices are the points of X. Two points $x, y \in X$ are connected by an edge if $B_r(x) \cap B_r(y) \neq \emptyset$.

Lemma 4.1. *Let ρ be the covering radius of X. If $r \geq \rho$, then the graph $\mathcal{G}_r$ is connected.*

Proof. Since $r \geq \rho$, the covering property

$$\bigcup_{x \in X} B_r(x) = \mathbb{S}^d$$

holds. We fix $x_0 \in X$ and consider its connected component $\mathcal{C}$, which consists of all vertices connected to x_0 by some path. The set $\mathbb{S}^d \setminus \bigcup_{x \in \mathcal{C}} B_r(x)$ is open since $\bigcup_{x \in \mathcal{C}} B_r(x)$ is closed. If $\mathbb{S}^d \setminus \bigcup_{x \in \mathcal{C}} B_r(x) \neq \emptyset$, then there is a sequence $(y_n)_{n \in \mathbb{N}} \subset \mathbb{S}^d \setminus \bigcup_{x \in \mathcal{C}} B_r(x)$ such that $y_n \to y \in \bigcup_{x \in \mathcal{C}} B_r(x)$. This means that $y \in B_r(x)$ for some $x \in \mathcal{C}$. Each y_n is contained in a spherical cap $B_r(x)$ for some $x \in X \setminus \mathcal{C}$. Since there are only finitely many, there is a subsequence y_{n_k} and some $\tilde{x} \in X \setminus \mathcal{C}$ such that $y_{n_k} \in B_r(\tilde{x})$ and $y_{n_k} \to y$. Consequently, for given $\epsilon > 0$ and k large enough,

$$\operatorname{dist}(\tilde{x}, x) \leq \operatorname{dist}(\tilde{x}, y_{n_k}) + \operatorname{dist}(y_{n_k}, y) + \operatorname{dist}(y, x) \leq r + \epsilon + r.$$

This implies $\operatorname{dist}(\tilde{x}, x) \leq 2r$ and, hence, $B_r(x) \cap B_r(\tilde{x}) \neq \emptyset$. Since $x \in \mathcal{C}$, then by definition of $\mathcal{G}_r$, also $\tilde{x} \in \mathcal{C}$. This, however, contradicts the earlier observation $\tilde{x} \in X \setminus \mathcal{C}$. Hence, we derive $\bigcup_{x \in \mathcal{C}} B_r(x) = \mathbb{S}^d$.

https://doi.org/10.1017/fms.2023.106 Published online by Cambridge University Press

Let $y \in X$ be arbitrary. By the covering property, $y \in B_r(x)$ for some $x \in \mathcal{C}$, and thus $B_r(y) \cap B_r(x) \neq \emptyset$. Consequently, $y \in \mathcal{C}$ and $\mathcal{C} = X$. This means that the graph $\mathcal{G}_r$ is connected, as claimed. □

4.2. Integration along the boundary of spherical caps

Due to (4), the boundary of a spherical cap $B_r(x)$ is

$$\begin{aligned} \partial B_r(x) &= \{z \in \mathbb{S}^d : \operatorname{dist}(x,z) = r\} \\ &= \{z \in \mathbb{S}^d : \langle x, z\rangle = \cos r\}. \end{aligned} \tag{26}$$

By the Pythagorian Theorem, $\partial B_r(x)$ is a $d-1$-dimensional Euclidean sphere of radius $\sin r$ centered at $x \cos r$ in a hyperplane perpendicular to x; that is,

$$\partial B_r(x) = \{z \in \mathbb{S}^d : \|x\cos r - z\| = \sin r\}. \tag{27}$$

It is the intersection of the sphere $\mathbb{S}^d$ with a suitable hyperplane, and we enforce the normalization

$$\int_{\partial B_r(x)} 1 = 1. \tag{28}$$

Next, we specify distinct functions that we integrate along $\partial B_r(x)$. Let $\mathcal{H}_k^d$ be the vector space of spherical harmonics of degree $k \in \mathbb{N}$ (i.e., the eigenspace of the Laplace-Beltrami operator on $\mathbb{S}^d$ with respect to the eigenvalue $-k(k+d-1)$, $k \in \mathbb{N}$; see, for example, [43] for background material). The dimension of $\mathcal{H}_k^d$ is

$$\dim(\mathcal{H}_k^d) = \frac{2k+d-1}{d-1}\binom{k+d-2}{d-2}, \tag{29}$$

and the orthogonality relations

$$\mathcal{H}_k^d \perp \mathcal{H}_l^d, \qquad k,l \in \mathbb{N}, \quad k \neq l, \tag{30}$$

hold. The space $\bigoplus_{k\le t} \mathcal{H}_k^d$ coincides with the restriction of Π_t to the sphere $\mathbb{S}^d$. When integrating over $\mathbb{S}^d$ or subsets or along curves in $\mathbb{S}^d$, we may therefore replace Π_t by $\bigoplus_{k\le t} \mathcal{H}_k^d$. The proofs of our main results in Sections 5 and 6 rely on the following key observation.

Lemma 4.2. *There are numbers $c_{d,k}(r) > 0$ such that*

$$\int_{\partial B_r(x)} f = c_{d,k}(r) f(x), \qquad \text{for all } f \in \mathcal{H}_k^d \text{ and } x \in \mathbb{S}^d. \tag{31}$$

In particular, the normalization (28) leads to $c_{d,0}(r) = 1$. The identity (31) is stated by Samko in [39, (1.37)] and referred to as a variant of the Cavalieri principle [39, Remark 4]. The analogue for the complex sphere is mentioned in [34].

Here we provide a new proof of Samko's formula that is based on an inductive construction of an orthonormal basis for $\mathcal{H}_k^d$. For these facts, we follow [32].

Proof. For $x \in \mathbb{S}^d$, we write

$$x = x_{d+1} e_{d+1} + \sqrt{1 - x_{d+1}^2}\,\bar{x}, \qquad \bar{x} \in \mathbb{S}^{d-1}.$$

https://doi.org/10.1017/fms.2023.106 Published online by Cambridge University Press

Let $\{X_l^{d-1,m}\}_{m=1}^{\dim(\mathcal{H}_l^{d-1})}$ be an orthonormal basis for $\mathcal{H}_l^{d-1}$. We denote the associated Legendre functions by $P_k^{d,l}$, $l = 0, \dots, k$, cf. [32]. Then

$$Y_k^{d,l,m}(x) = P_k^{d,l}(x_{d+1}) X_l^{d-1,m}(\bar{x}), \qquad l = 0, \dots, k, \quad m = 1, \dots, \dim(\mathcal{H}_l^{d-1}),$$

form an orthogonal basis [2] for $\mathcal{H}_k^d$ and

$$Y_k^{d,l,m}(e_{d+1}) = a_{d,k}\delta_{l,0}, \tag{32}$$

with suitable normalization constants $a_{d,k}$, cf. [32, Lemma 15].

We first verify that $\int_{\partial B_r(x)} f = c_{d,k}(r) f(x)$ for $x = e_{d+1}$. In this case, $\partial B_r(e_{d+1}) = \{(z' \sin r, \cos r) : z' \in \mathbb{S}^{d-1}\}$, and the homogeneity of $X_l^{d-1,m}$ yields

$$\begin{aligned}\int_{\partial B_r(e_{d+1})} Y_k^{d,l,m} &= P_k^{d,l}(\cos r) \int_{\mathbb{S}^{d-1}} X_l^{d-1,m}(\sin r \cdot) \\ &= P_k^{d,l}(\cos r) \sin^l r \int_{\mathbb{S}^{d-1}} X_l^{d-1,m} \\ &= P_k^{d,0}(\cos r) \sin^l r \ \delta_{l,0}.\end{aligned}$$

After comparing with (32), we set $c_{d,k}(r) := P_k^{d,0}(\cos r) \sin^l r / a_{d,k}$ and obtain

$$\int_{\partial B_r(e_{d+1})} Y_k^{d,l,m} = c_{d,k}(r) Y_k^{d,l,m}(e_{d+1}).$$

For $k = 0$, $Y_0^{d,0,0}$ is constant, and the normalization $\int_{\partial B_r(e_{d+1})} 1 = 1$ implies that $c_{d,0}(r) = 1$ for all r. Thus we have verified that (31) holds for all $f \in \mathcal{H}_l^d$ and $x = e_{d+1}$.

We now consider general $x \in \mathbb{S}^d$. There is a rotation matrix O such that $x = Oe_{d+1}$ and $\partial B_r(x) = \partial B_r(Oe_{d+1}) = O\partial B_r(e_{d+1})$. This leads to

$$\int_{\partial B_r(x)} f = \int_{O\partial B_r(e_{d+1})} f = \int_{\partial B_r(e_{d+1})} f \circ O.$$

Since $\mathcal{H}_l^d$ is orthogonally invariant, $f \circ O \in \mathcal{H}_l^d$ and our observations for e_{d+1} imply

$$\int_{\partial B_r(x)} f = c_{d,k}(r)(f \circ O)(e_{d+1}) = c_{d,k}(r) f(x). \qquad \square$$

On $\mathbb{S}^2$ Samko's formula connects point evaluations to line integrals and thus gives a first hint of how quadrature formulas might be related to t-design curves.

5. Asymptotically optimal t-design curves in $\mathbb{S}^2$

We now state our first main result, which is Theorem 1.2 of the Introduction.

Theorem 5.1. *There is a sequence of asymptotically optimal t-design curves in $\mathbb{S}^2$; that is, there exists a sequence of piecewise smooth, closed curves $\gamma_t : [0,1] \to \mathbb{S}^2$, for $t \in \mathbb{N}$, of length $\ell(\gamma_t) \asymp t$, such that*

$$\frac{1}{\ell(\gamma_t)} \int_{\gamma_t} f = \int_{\mathbb{S}^2} f \qquad \text{for all } f \in \Pi_t .$$

The trajectory of every γ_t is a union of Euclidean circles.

[2] Note that for the next step of the induction, we need to relabel the $Y_k^{d,l,m}$ as $X_l^{d,m}$.

https://doi.org/10.1017/fms.2023.106 Published online by Cambridge University Press

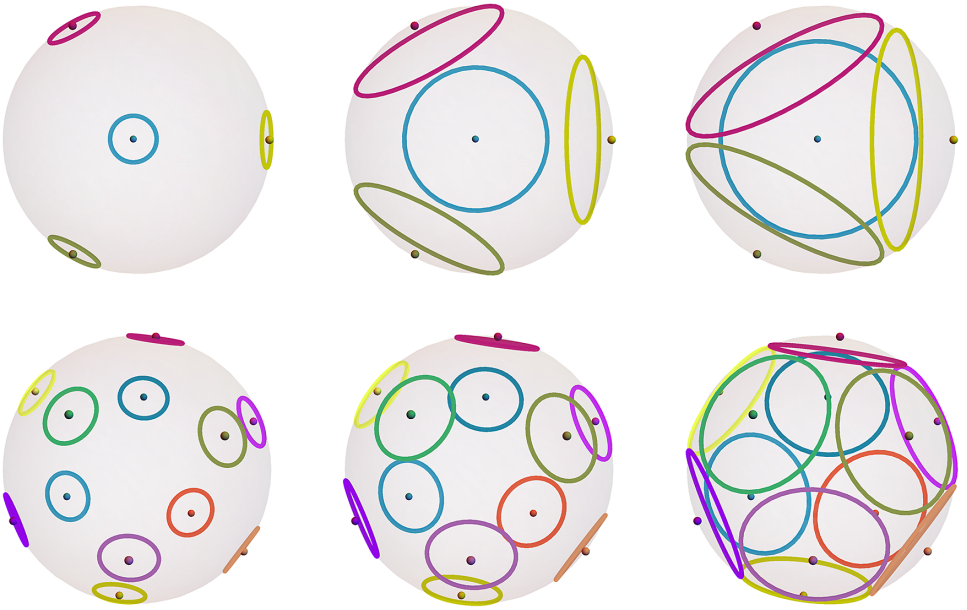

Figure 2. *Circles centered at t-design points with radii increasing from left to right. The top row shows 2-design points and the bottom row 5-design points.*

Proof. According to (27) with $d = 2$, the boundary of the spherical cap $B_r(x) = \{z \in \mathbb{S}^2 : \operatorname{dist}(x, z) \le r\}$ is a Euclidean circle of radius $\sin r$ given by

$$\Gamma_{x,r} = \{z \in \mathbb{S}^2 : \|x \cos r - z\| = \sin r\} \subset \mathbb{S}^2, \tag{33}$$

cf. Figure 2. The asymptotically optimal t-design curve will be constructed from a union of circles $\Gamma_{x,r}$, where x runs through a set of t-design points and r is essentially their covering radius. For each circle, we choose an (arbitrary) orientation and obtain a closed curve $\gamma_{x,r}$ with trajectory $\Gamma_{x,r}$. The formal sum $\gamma_t^r = \dot{+}_{x \in X_t} \gamma_{x,r}$ is usually called a cycle with trajectory $\bigcup_{x \in X_t} \Gamma_{x,r}$ and integral $\int_{\gamma_t^r} f = \sum_{x \in X_t} \int_{\gamma_{x,r}} f$ [38].

Note that in $\mathbb{S}^2$ the submanifold $\partial B_r(x)$ and the circle $\Gamma_{x,r}$ coincide, so that the normalization (28) leads to $\int_{\Gamma_{x,r}} f = \frac{1}{\ell(\gamma_{x,r})} \int_{\gamma_{x,r}} f$, where $\gamma_{x,r}$ is the actual curve that traverses $\Gamma_{x,r}$. In higher dimensions, this slight inconsistency between $\Gamma_{x,r}$ and $\partial B_r(x)$ no longer occurs.

(i) According to [3], there is a sequence $(X_t)_{t \in \mathbb{N}}$ of asymptotically optimal t-design points in $\mathbb{S}^2$; that is, there exist finite sets $X_t \subset \mathbb{S}^2$, such that $|X_t| \asymp t^2$ and

$$\frac{1}{|X_t|} \sum_{x \in X_t} f(x) = \int_{\mathbb{S}^2} f, \qquad \text{for all } f \in \bigoplus_{k \le t} \mathcal{H}_k^2 . \tag{34}$$

(ii) Let $r > 0$, $\Gamma_t^r := \bigcup_{x \in X_t} \Gamma_{x,r}$, and $\gamma_t^r := \dot{+}_{x \in X_t} \gamma_{x,r}$ be the corresponding cycle. We first show that this cycle provides exact integration on Π_t.

For the component $\mathcal{H}_0^2 = \operatorname{span}\{1\}$, we observe

$$\frac{1}{\ell(\gamma_t^r)} \int_{\gamma_t^r} 1 = 1 = \int_{\mathbb{S}^d} 1.$$

https://doi.org/10.1017/fms.2023.106 Published online by Cambridge University Press

We now consider $f \in \mathcal{H}_k^2$ for $1 \le k \le t$. Lemma 4.2 with $c_k(r) := c_{2,k}(r)$ and the definition of t-design points yields

$$\begin{aligned}\frac{1}{\ell(\gamma_t^r)}\int_{\gamma_t^r} f &= \frac{1}{|X_t|}\sum_{x\in X_t}\frac{1}{\ell(\gamma_{x,r})}\int_{\gamma_{x,r}} f \\ &= \frac{1}{|X_t|}\sum_{x\in X_t}\int_{\Gamma_{x,r}} f \\ &= \frac{c_k(r)}{|X_t|}\sum_{x\in X_t} f(x) \\ &= c_k(r)\int_{\mathbb{S}^2} f.\end{aligned}$$

Since $\mathcal{H}_0^2 \perp \mathcal{H}_k^2$ for $k = 1, 2, \ldots$, cf. (30), we obtain $\int_{\mathbb{S}^2} f = 0$ for $f \in \mathcal{H}_k^2$, and the factor $c_k(r)$ does not matter. We derive

$$\frac{1}{\ell(\gamma_t^r)}\int_{\gamma_t^r} f = \int_{\mathbb{S}^2} f \qquad \text{for all } f \in \mathcal{H}_k^2, \tag{35}$$

and, by linearity, exact quadrature holds for all $f \in \bigoplus_{k=0}^t \mathcal{H}_k^2$.

(iii) Identity (35) holds for every $0 < r < \frac{\pi}{2}$, and thus every cycle γ_t^r (formal sum of closed curves) yields exact integration. We now determine radii $r = r_t$ depending on the degree t, so that $\Gamma_t := \Gamma_t^{r_t} = \bigcup_{x\in X_t}\Gamma_{x,r_t}$ is indeed the trajectory of a single continuous closed curve.

Let $\rho_t = \sup_{x\in\mathbb{X}}\big(\inf_{y\in X_t}\operatorname{dist}_{\mathbb{X}}(x,y)\big)$ be the covering radius of X_t as in (9). We choose $r_t := \rho_t$, so that

$$\mathbb{S}^2 = \bigcup_{x\in X_t} B_{r_t}(x). \tag{36}$$

The circles $\Gamma_{x,r_t} = \partial B_{r_t}(x)$, for $x \in X_t$, induce a graph $\mathcal{G}$ as follows: the vertices of $\mathcal{G}$ are the intersection points of the Γ_{x,r_t}, and its edges are associated to arcs on these circles between the intersection points, cf. Figures 2 and 3. For each circle Γ_{x,r_t}, we have fixed an orientation. As a result of this construction, we obtain a directed graph $\mathcal{G}_{\rightarrow}$ [47].

Lemma 5.2. *The graph $\mathcal{G}$ is strongly connected (i.e., the directed graph $\mathcal{G}_{\rightarrow}$ is connected).*

Proof. We first verify that the undirected graph $\mathcal{G}$ is connected. Pick two arbitrary but distinct vertices $v_1, v_2 \in \mathcal{G}$. Then there are points $x_1, x_2 \in X_t$ such that $v_i \in \partial B_{r_t}(x_i)$ for $i = 1, 2$. If $x_1 = x_2$, then v_1, v_2 are connected in $\mathcal{G}$ since they lie on the same circle.

We may thus assume that $x_1 \neq x_2$. In this case, we consider the auxiliary graph $\mathcal{G}_{r_t}$ treated in Lemma 4.1. Its vertices are the points of the t-design X_t. Two points $x, y \in X_t$ are connected by an edge if and only if $B_{r_t}(x) \cap B_{r_t}(y) \neq \emptyset$. According to Lemma 4.1 and $r_t \ge \rho_t$, the graph $\mathcal{G}_{r_t}$ is connected. Thus, there is a path from x_1 to x_2 in $\mathcal{G}_{r_t}$, say $x_1 = x_{i_1}, \ldots, x_{i_m} = x_2$, so that $B_{r_t}(x_{i_j}) \cap B_{r_t}(x_{i_{j+1}}) \neq \emptyset$. This also implies $\partial B_{r_t}(x_{i_j}) \cap \partial B_{r_t}(x_{i_{j+1}}) \neq \emptyset$. Clearly, vertices $v_{i_j}, v_{i_{j+1}}$ of $\mathcal{G}$ with $v_{i_j} \in \partial B_{r_t}(x_{i_j})$ and $v_{i_{j+1}} \in \partial B_{r_t}(x_{i_{j+1}})$ are connected in $\mathcal{G}$. Eventually, there is a path from v_1 to v_2 in $\mathcal{G}$.

We still need to verify that the directed graph $\mathcal{G}_{\rightarrow}$ is also connected. If two distinct vertices $v_{i_j}, v_{i_{j+1}}$ lie on the same circle $\partial B_{r_t}(x_1)$, then we simply get from v_{i_j} to $v_{i_{j+1}}$ by following the chosen orientation of $\partial B_{r_t}(x_1)$. No further difficulties arise, and we deduce that $\mathcal{G}_{\rightarrow}$ is connected. □

By construction, each vertex of $\mathcal{G}_{\rightarrow}$ has as many incoming as outgoing edges, cf. Figure 3. Euler's Theorem about directed, strongly connected graphs implies that there is an Euler cycle [47]. Hence, all circles in $\bigcup_{x\in X_t}\partial B_{r_t}(x) = \bigcup_{x\in X_t}\Gamma_{x,r_t}$ can be traversed by a single, closed, piecewise smooth curve γ_t on $\mathbb{S}^2$ with trajectory $\Gamma_t = \bigcup_{x\in X_t}\Gamma_{x,r_t}$.

https://doi.org/10.1017/fms.2023.106 Published online by Cambridge University Press

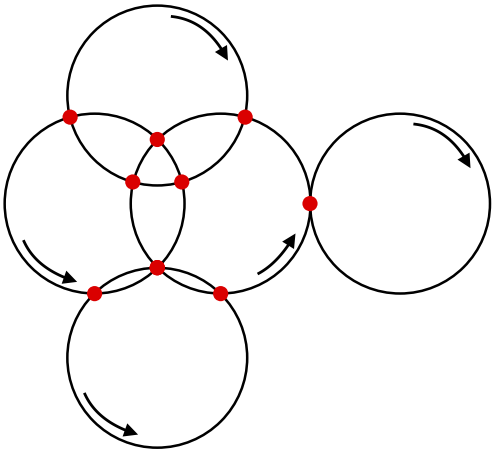

Figure 3. *A set of connected circles induces a directed graph, whose vertices are the intersection points and whose edges are the associated arcs of the circles. Each vertex has equal in-degree and out-degree, namely, the number of circles running through this point.*

(iv) To compute the length of γ_t, we relate the covering radius r_t of X_t to the degree t. The same proof as in (13) shows that $r_t \lesssim t^{-1}$; see also [4, 6]. Therefore, $\ell(\gamma_{x,r_t}) = 2\pi \sin r_t \asymp r_t \lesssim t^{-1}$. This leads to

$$\ell(\gamma_t) = |X_t|\ell(\gamma_{x,r_t}) \asymp t^2 r_t \lesssim t.$$

In view of the lower bound for the length of t-design curves in Theorem 2.2, our construction yields a sequence of asymptotically optimal t-design curves. □

6. General existence of spherical t-design curves

We now prove the existence of t-design curves in $\mathbb{S}^d$ for all $t \in \mathbb{N}$ in dimension $d \geq 2$. This is Theorem 1.3 of the Introduction.

Theorem 6.1. *Let $d \geq 2$ be an arbitrary integer. There is a sequence $(\gamma_t)_{t\in\mathbb{N}}$ of t-design curves in $\mathbb{S}^d$ such that*

$$\ell(\gamma_t) \lesssim t^{\frac{d(d-1)}{2}}.$$

Furthermore, the trajectory of every γ_t consists of a union of Euclidean circles.

We will prove this theorem by induction on the dimension d. Similar to the proof of Theorem 5.1, we first show the existence of a cycle (a formal sum of closed curves) that yields exact integration. Then we use a combinatorial argument to build a connected trajectory.

6.1. Some geometry on the sphere

Let us first state few simple observations about the action of the orthogonal group on $\mathbb{S}^d$.

Lemma 6.2. *Let $d \geq 2$ and $A, B \subseteq \mathbb{R}^d$ be two finite sets. If $0 \notin A$, then there is a rotation $O \in \mathcal{O}(d)$ such that $OA \cap B = \emptyset$.*

Proof. For the sake of completeness, we provide the simple arguments.

The claim is verified by induction. For the induction step, we identify $\mathcal{O}(d)$ as a subgroup of $\mathcal{O}(d+1)$ via the homomorphism $\bar{O} \in \mathcal{O}(d) \mapsto j(\bar{O}) \in \mathcal{O}(d+1)$, $j(\bar{O})(x) = (\bar{O}\bar{x}, x_{d+1})$ for $x = (\bar{x}, x_{d+1}) \in \mathbb{R}^{d+1}$.

https://doi.org/10.1017/fms.2023.106 Published online by Cambridge University Press

The case $d = 2$ is obvious. Consider now $A, B \subseteq \mathbb{R}^{d+1}$. Let $\bar{A}, \bar{B} \subseteq \mathbb{R}^d$ be the orthogonal projections of A, B onto the first d coordinates.

Case 1: $0 \notin \bar{A}$. By the induction hypothesis, there exists $\bar{O} \in \mathcal{O}(d)$ such that $\bar{O}\bar{A} \cap \bar{B} = \emptyset$. Then $O = j(\bar{O}) \in \mathcal{O}(d+1)$ satisfies $OA \cap B = \emptyset$.

Case 2: $0 \in \bar{A}$. Since $0 \notin A$, there is $O_1 \in \mathcal{O}(d+1)$ such that $\overline{O_1 A} \cap (\mathbb{R}e_{d+1}) = \emptyset$. Let $A_1 = O_1 A$ and $\bar{A}_1$ be the projection onto the first d coordinates. Then $0 \notin \overline{O_1 A}$, and by the induction hypothesis there is $\bar{O}_2 \in \mathcal{O}(d)$ such that $\bar{O}_2 \overline{A_1} \cap \bar{B} = \emptyset$. Then $O = j(\bar{O}_2) O_1$ satisfies $OA \cap B = \emptyset$. □

Corollary 6.3. *Let $d \geq 2$, $v \in \mathbb{S}^d$ and $A, B \subseteq \mathbb{S}^d$ two finite sets. If $\pm v \notin A$, then there is a rotation $O \in \mathcal{O}(d+1)$ such that $Ov = v$ and $OA \cap B = \emptyset$.*

Proof. Without loss of generality, we may assume that $v = e_{d+1} \in \mathbb{S}^d$. Let $\bar{A}, \bar{B} \subseteq \mathbb{R}^d$ be the orthogonal projections of A, B onto the first d coordinates. Since $\pm e_{d+1} \notin A$, we deduce $0 \notin \bar{A}$. According to Lemma 6.2, there is $\bar{O} \in \mathcal{O}(d)$ such that $\bar{O}\bar{A} \cap \bar{B} = \emptyset$. The $O = j(\bar{O}) \in \mathcal{O}(d+1)$ does the job. □

As in Section 4, we now consider spherical caps and their boundary

$$B_r(x) = \{y \in \mathbb{S}^d : \operatorname{dist}_{\mathbb{S}^d}(x, y) \leq r\},$$
$$\partial B_r(x) = \{z \in \mathbb{S}^d : \|x \cos \rho_t - z\| = \sin r\};$$

see (33) for $d = 2$. Clearly, $\partial B_r(x)$ is homeomorphic (diffeomorphic) to the $d-1$-dimensional sphere $\mathbb{S}^{d-1}$. For our analysis, we will use the following homeomorphism.

Let $x \in \mathbb{S}^d$, $0 < r < \frac{\pi}{2}$ and $O = O_x \in \mathcal{O}(d+1)$ a matrix in the orthogonal group acting on $\mathbb{R}^{d+1}$ such that $x = Oe_{d+1}$, where $e_{d+1} = (0, \dots, 0, 1)^\top \in \mathbb{R}^{d+1}$. Now set

$$\phi_{x,r}(z) = O\begin{pmatrix} \sin r z \\ \cos r \end{pmatrix}, \qquad z \in \mathbb{S}^{d-1}, \tag{37}$$

and recall that $e_d \in \mathbb{R}^d$ is the north pole in $\mathbb{S}^{d-1}$.

Lemma 6.4. *The map $\phi_{x,r} : \mathbb{S}^{d-1} \to \mathbb{S}^d$ has the following properties.*

(i) *$\phi_{x,r}$ is a diffeomorphism between $\mathbb{S}^{d-1}$ and $\partial B_r(x)$.*

(ii) *Let $x, y \in \mathbb{S}^{d-1}$ with $\operatorname{dist}_{\mathbb{S}^d}(x, y) < r \leq \frac{\pi}{2}$. Then there is a unique radius $\sigma \in [\pi/3, \pi/2]$, such that*

$$\phi_{x,r}\big(\partial B_\sigma(e_d)\big) = \partial B_r(x) \cap \partial B_r(y)\,.$$

In particular, the intersection $\partial B_r(x) \cap \partial B_r(y)$ is diffeomorphic to $\mathbb{S}^{d-2}$.

Proof of Lemma 6.4. (i) If $\|z\| = 1$, then $\|\phi_{x,r}(z)\|^2 = \|z\|^2 \sin^2 r + \cos^2 r = 1$, and

$$\begin{aligned} \operatorname{dist}(x, \phi_{x,r}(z)) &= \operatorname{dist}(Oe_{d+1}, O(z \sin r, \cos r) \\ &= \arccos\langle e_{d+1}, (z \sin r, \cos r)\rangle = r\,. \end{aligned}$$

Clearly, $\phi_{x,r}$ is a bijection between $\mathbb{S}^{d-1}$ and $\partial B_r(x)$.

(ii) For $z \in \mathbb{R}^{d+1}$, we write $z = (z', z_{d+1}) = (z'', z_d, z_{d+1})$ with $z' \in \mathbb{R}^d$ and $z'' \in \mathbb{R}^{d-1}$. By applying a suitable rotation, we may assume without loss of generality that $x = e_{d+1}$ and $y = \sqrt{1 - y_{d+1}^2}\, e_d + y_{d+1} e_{d+1} = (0, \sqrt{1 - y_{d+1}^2}, y_{d+1})$. Then the assumption $\operatorname{dist}(x, y) = \arccos\langle x, y\rangle < r$ yields $\langle x, y\rangle = y_{d+1} > \cos r$.

Now take $z \in \partial B_r(e_{d+1}) \cap \partial B_r(y)$. By Step (i),

$$\partial B_r(e_{d+1}) = \phi_{e_{d+1},r}(\mathbb{S}^{d-1}) = \{(z' \sin r, \cos r : z' \in \mathbb{S}^{d-1}\},$$

https://doi.org/10.1017/fms.2023.106 Published online by Cambridge University Press

so $z_{d+1} = \cos r$. Since $\operatorname{dist}(z, y) = \arccos\langle z, y\rangle = r$ as well, we obtain

$$\langle z, y\rangle = z_d\sqrt{1 - y_{d+1}^2} + z_{d+1}y_{d+1} = z_d\sqrt{1 - y_{d+1}^2} + \cos r\, y_{d+1} = \cos r\,.$$

Solving for z_d, this implies that

$$z_d = \cos r\,\frac{1 - y_{d+1}}{\sqrt{1 - y_{d+1}^2}}\,. \tag{38}$$

Let us abbreviate the occurring fraction by $\tau = \frac{1-y_{d+1}}{\sqrt{1-y_{d+1}^2}}$. Then

$$\begin{aligned}\|z''\|^2 &= 1 - z_{d+1}^2 - z_d^2\\ &= 1 - \cos^2 r - \tau^2\cos^2 r\\ &= \sin^2 r - \tau^2\cos^2 r =: s^2\,.\end{aligned} \tag{39}$$

We may switch from z'' to sz'' with $z'' \in \mathbb{S}^{d-2}$, so that every point in $z \in \partial B_r(x) \cap \partial B_r(y)$ has coordinates

$$z = \begin{pmatrix} sz'' \\ \tau\cos r \\ \cos r\end{pmatrix}, \qquad z'' \in \mathbb{S}^{d-2}\,. \tag{40}$$

By comparison, a point $z' \in \partial B_\sigma(e_d) \subseteq \mathbb{S}^{d-1}$ is of the form $(z''\sin\sigma, \cos\sigma)$ for $z'' \in \mathbb{S}^{d-2}$. Consequently,

$$\phi_{e_{d+1},r}(z') = \begin{pmatrix} z''\sin\sigma\,\sin r \\ \cos\sigma\,\sin r \\ \cos r\end{pmatrix}. \tag{41}$$

We have to show that every point in $\partial B_r(x) \cap \partial B_r(y)$ can be represented in this way. For (40) and (41) to represent the same set, we need to verify that the following identities

$$s = \sin\sigma\,\sin r \qquad \text{and} \qquad \cos r\,\tau = \cos\sigma\,\sin r \tag{42}$$

can be satisfied with a suitable choice of σ. Clearly, σ is determined by

$$\sin\sigma = \frac{s}{\sin r}\,. \tag{43}$$

Then using (39),

$$\cos^2\sigma\,\sin^2 r = (1 - \sin^2\sigma)\sin^2 r = \sin^2 r - s^2 = \tau^2\,\cos^2 r\,,$$

and the second identity in (42) is also satisfied.

Finally, since $y_{d+1} = \cos r$ and $\tau^2 = \frac{1-y_{d+1}}{1+y_{d+1}}$, we estimate the size of σ as

$$\begin{aligned}\sin^2\sigma = \frac{s^2}{\sin^2 r} &= 1 - \frac{\cos^2 r}{\sin^2 r}\,\frac{1 - y_{d+1}}{1 + y_{d+1}}\\ &\geq 1 - \frac{\cos^2 r}{\sin^2 r}\,\frac{1 - \cos r}{1 + \cos r}\,.\end{aligned}$$

https://doi.org/10.1017/fms.2023.106 Published online by Cambridge University Press

For $u = \cos r \geq 0$, we observe

$$1 - \frac{\cos^2 r}{\sin^2 r}\,\frac{1-\cos r}{1+\cos r} = 1 - \frac{u^2}{1-u^2}\,\frac{1-u}{1+u} = 1 - \frac{u^2}{(1+u)^2} \geq \frac{3}{4},$$

so that we obtain $\sin^2 \sigma \geq \frac{3}{4}$. Consequently, $\pi/3 \leq \sigma \leq \pi/2$, which means that $B_\sigma(e_d)$ covers a fixed portion of $\mathbb{S}^{d-1}$. □

Next, we check how curves in $\mathbb{S}^{d-1}$ – in particular, t-design curves – are mapped by $\phi_{x,r}$.

Lemma 6.5. *Suppose that γ is a t-design curve in $\mathbb{S}^{d-1}$. Let $x \in \mathbb{S}^d$ and $0 < r < \frac{\pi}{2}$.*

(i) *Then $\gamma_{x,r} = \phi_{x,r} \circ \gamma$ is a curve in $\partial B_r(x) \subseteq \mathbb{S}^d$ with length $\ell(\gamma_{x,r}) = \ell(\gamma)\,\sin r$, such that*

$$\frac{1}{\ell(\gamma_{x,r})} \int_{\gamma_{x,r}} f = \int_{\partial B_r(x)} f, \qquad \text{for all } f \in \Pi_t\,.$$

(ii) *For a given point $w \in \partial B_r(x)$, there is a t-design curve γ' in $\mathbb{S}^{d-1}$, such that w lies on $\phi_{x,r} \circ \gamma'$.*
(iii) *If γ consists a union of circles, then so does $\gamma_{x,r}$ and γ' can also be chosen to do so.*
(iv) *Assume that γ and $\Psi \subseteq \mathbb{S}^d$ both consist of a finite union of circles and $w \in \Psi$. Then there exists a t-design curve γ'' in $\mathbb{S}^{d-1}$ consisting of a union of circles, such that w is contained in the trajectory $\Gamma''_{x,r}$ of the curve $\phi_{x,r} \circ \gamma''$ and the intersection $\Gamma''_{x,r} \cap \Psi$ is finite.*

In the following, we refer to $\gamma_{x,r}$ as a t-design curve for $\partial B_r(x)$.

Proof. (i) First we consider the north pole $x = e_{d+1}$. The curve $\gamma_{e_{d+1},r} = \phi_{e_{d+1},r} \circ \gamma = (\gamma\,\sin r, \cos r)^\top$ has arc length $\ell(\gamma_{e_{d+1},r}) = \sin r\,\ell(\gamma)$, and we derive

$$\begin{aligned}\frac{1}{\ell(\gamma_{e_{d+1},r})} \int_{\gamma_{e_{d+1},r}} f &= \frac{1}{\sin r\,\ell(\gamma)} \int_0^1 f(\gamma(s)\,\sin r, \cos r) \| \sin r\,\dot\gamma(s)\| \mathrm{d}s \\ &= \frac{1}{\ell(\gamma)} \int_\gamma f(\,\cdot\,\sin r, \cos r).\end{aligned}$$

The last integral $\int_\gamma$ is the line integral of the function $y \in \mathbb{S}^{d-1} \mapsto f \circ \phi_{e_{d+1},r}(y) = f(y \sin r, \cos r)$ along γ in $\mathbb{S}^{d-1}$. For $f \in \Pi_t$ and $y \in \mathbb{S}^{d-1}$, the function $f(y \sin r, \cos r)$ is a polynomial of degree t restricted to $\mathbb{S}^{d-1}$. The t-design property leads to

$$\begin{aligned}\frac{1}{\ell(\gamma_{e_{d+1},r})} \int_{\gamma_{e_{d+1},r}} f &= \int_{\mathbb{S}^{d-1}} f(\sin r\,\cdot\,, \cos r) \\ &= \int_{\partial B_r(e_{d+1})} f\,,\end{aligned}$$

where the latter equality is due to the normalization $\int_{\mathbb{S}^{d-1}} 1 = 1 = \int_{\partial B_r(e_{d+1})} 1$, cf. (28).

For general $x \in \mathbb{S}^d$, there is a rotation matrix O such that $x = Oe_{d+1}$ and rotational invariance of the distance function on $\mathbb{S}^d$ yields $B_r(x) = OB_r(e_{d+1})$ and $\partial B_r(x) = O\partial B_r(e_{d+1})$. The curve $\gamma_{x,r} = O\gamma_{e_{d+1},r} = \phi_{x,r} \circ \gamma$ satisfies $\|\dot\gamma_{x,r}\| = \|\dot\gamma_{e_{d+1},r}\|$. For $f \in \Pi_t$, we also have $f \circ O \in \Pi_t$ and deduce

$$\begin{aligned}\int_{\partial B_r(x)} f = \int_{O\partial B_r(e_{d+1})} f &= \int_{\partial B_r(e_{d+1})} f \circ O \\ &= \frac{1}{\ell(\gamma_{e_{d+1},r})} \int_{\gamma_{e_{d+1},r}} f \circ O = \frac{1}{\ell(\gamma_{x,r})} \int_{\gamma_{x,r}} f.\end{aligned}$$

https://doi.org/10.1017/fms.2023.106 Published online by Cambridge University Press

(ii) If γ is a t-design curve in $\mathbb{S}^{d-1}$, then for every orthogonal matrix $U \in \mathcal{O}(d)$ the rotated curve $\gamma' = U\gamma$ is also a t-design curve in $\mathbb{S}^{d-1}$. By suitably choosing U, we can always achieve that a given point $v \in \mathbb{S}^{d-1}$ lies on the trajectory of $U\gamma$. Now let $w \in \partial B_r(x) \subseteq \mathbb{S}^d$ and $v \in \mathbb{S}^{d-1}$ its pre-image under $\phi_{x,r}$. Consequently, $w = \phi_{x,r}(v)$ lies on the curve $\gamma'_{x,r} = \phi_{x,r} \circ (U\gamma)$.

(iii) Clearly, if γ is a union of (Euclidean) circles in $\mathbb{S}^{d-1}$, then $\gamma_{x,r} = O(\sin r\, \gamma, \cos r)^\top$ is a union of Euclidean circles in $\mathbb{S}^d$. The same holds for $\gamma' = U\gamma$.

(iv) Let $v = \phi_{x,r}^{-1}(w)$ and let $\Psi_0 = \phi_{x,r}^{-1} \circ (\Psi \cap \partial B_r(x))$. Then Ψ_0 is again a finite union of circles or arcs of circles. Two circles are either disjoint, or they intersect in one or two points, or they coincide. This can happen only when the two circles have the same center. Let $C_\gamma \subseteq \mathbb{S}^{d-1}$ be the set of centers of the circles of the given curve γ and C_{Ψ_0} be the centers of Ψ_0 (including centers of parts of circles).

We may assume that $\pm v \notin C_\gamma$ (otherwise apply a rotation to γ).

Since C_γ and C_{Ψ_0} are both finite and $\pm v \notin C_\gamma$, Corollary 6.3 yields an orthogonal matrix $U \in \mathcal{O}(d)$ such that $Uv = v$ and

$$UC_\gamma \cap C_{\Psi_0} = \emptyset\,.$$

The curve $\gamma'' = U\gamma$ consists of circles whose centers are disjoint from those of Ψ_0; consequently, γ'' and Ψ_0 have only finitely many points in common. After mapping via $\phi_{x,r}$, we obtain a trajectory $\Gamma''_{x,r} = \phi_{x,r} \circ \gamma''$ in $\mathbb{S}^d$ consisting of circles, such that $w \in \Gamma''_{x,r}$ and $\Gamma''_{x,r} \cap \Psi$ is finite. □

Lemma 6.6. *Let γ be a closed curve in $\mathbb{S}^d$ with trajectory Γ, so that its covering radius satisfies $r < \pi/4$. Then Γ intersects the boundary $\partial B_\sigma(x)$ for all $x \in \mathbb{S}^{d-1}$ and $\sigma \in (\pi/4, \pi/2)$:*

$$\Gamma \cap \partial B_\sigma(x) \neq \emptyset\,.$$

Proof. Since the covering radius of Γ is $r < \pi/4$, there exists a point $z \in \Gamma$, such that $\operatorname{dist}(z, x) \leq r$, and thus, $z \in B_r(x) \subseteq B_\sigma(x)$. Similarly, there exists a point $\tilde{z} \in \Gamma$, such that $\operatorname{dist}(\tilde{z}, -x) \leq r$, and thus, $\tilde{z} \in B_r(-x) \subseteq B_\sigma(-x)$. Since

$$\pi = \operatorname{dist}(x, -x) \leq \operatorname{dist}(x, \tilde{z}) + \operatorname{dist}(\tilde{z}, -x)\,,$$

we see that $\operatorname{dist}(\tilde{z}, x) \geq \pi - r \geq \sigma$ and $\tilde{z} \notin B_\sigma(x)$. Consequently, the continuous function $\psi(s) = \operatorname{dist}(\gamma(s), x)$ takes values $< \sigma$ and $> \sigma$. As a consequence, there exists s_0, such that $\psi(s_0) = \operatorname{dist}(\gamma(s_0), x) = \sigma$. In other words, the point $\gamma(s_0)$ is in $\partial B_\sigma(x)$ or $\Gamma \cap \partial B_\sigma(x) \neq \emptyset$. □

By combining Lemma 6.5 with Lemma 4.2, we obtain that

$$\frac{1}{\ell(\gamma_{x,r})} \int_{\gamma_{x,r}} f = \int_{\partial B_r(x)} f = c_{d,k}(r) f(x) \qquad \text{for all } f \in \mathcal{H}_k^d\,. \tag{44}$$

As in Section 5, this formula paves the way to make a transition from t-design points to t-design curves.

6.2. Part I of the proof of Theorem 6.1

Proof. We first prove the existence of a cycle (a formal sum of closed, piecewise smooth curves) in $\mathbb{S}^d$ that yields exact integration for Π_t. We prove this claim by induction on the dimension d. The case $d = 2$ corresponds to Theorem 5.1 and shows that the optimal design curve can be realized as a union of circles. We now assume that the claim holds for $d - 1$ with unions of circles.

For $0 < r < \frac{\pi}{2}$ and $x \in \mathbb{S}^d$, the induction hypothesis combined with Lemma 6.5(i) shows that there is a sequence of t-design curves $\left(\gamma_{x,r,t}\right)_{t \in \mathbb{N}}$ for $\partial B_r(x)$ of length

$$\ell(\gamma_{x,r,t}) \lesssim \sin r\, t^{\frac{(d-1)(d-2)}{2}}\,, \tag{45}$$

whose trajectories $\Gamma_{x,r,t} = \gamma_{x,r,t}([0,1])$ consist of unions of circles.

https://doi.org/10.1017/fms.2023.106 Published online by Cambridge University Press

As in the proof of Theorem 5.1, we use a sequence $(X_t)_{t\in\mathbb{N}}$ of asymptotically optimal t-design points in $\mathbb{S}^d$ and verify that the cycle $\gamma_t^r = \dot{+}_{x\in X_t}\gamma_{x,r,t}$ associated to the trajectory $\Gamma_t^r := \bigcup_{x\in X_t}\Gamma_{x,r,t}$ provides an exact quadrature on Π_t. A careful choice of the radius r will then yield a single closed curve instead of a cycle.

For the component $\mathcal{H}_0^2 = \operatorname{span}\{1\}$, we observe

$$\frac{1}{\ell(\gamma_t^r)}\int_{\gamma_t^r} 1 = 1 = \int_{\mathbb{S}^d} 1.$$

Next, we consider $f \in \mathcal{H}_k^d$ for $1 \le k \le t$. On the one hand, since $\ell(\gamma_r^t) = |X_t|\ell(\gamma_{x,r,t})$, Lemma 6.5(i) yields

$$\begin{aligned}\frac{1}{\ell(\gamma_t^r)}\int_{\gamma_t^r} f &= \frac{1}{|X_t|}\sum_{x\in X_t}\frac{1}{\ell(\gamma_{x,r,t})}\int_{\gamma_{x,r,t}} f \\ &= \frac{1}{|X_t|}\sum_{x\in X_t}\int_{\partial B_r(x)} f.\end{aligned}$$

On the other hand, by Lemma 4.2 for $f \in \mathcal{H}_k^d$, we have

$$\frac{1}{|X_t|}\sum_{x\in X_t}\int_{\partial B_r(x)} f = c_{d,k}(r)\frac{1}{|X_t|}\sum_{x\in X_t} f(x) = c_{d,k}(r)\int_{\mathbb{S}^d} f = 0 = \int_{\mathbb{S}^d} f\,.$$

In combination, we obtain

$$\frac{1}{\ell(\gamma_t^r)}\int_{\gamma_t^r} f = \int_{\mathbb{S}^d} f$$

for all $f \in \bigoplus_{k=0}^t \mathcal{H}_k^d$. This concludes the first part of the proof. □

6.3. *Part II of the proof of Theorem 6.1: Existence of a single closed curve*

If r is too small, then the trajectory Γ_t^r is not connected. If r is too big, then we may not match the desired asymptotics $\ell(\Gamma_t^r) \lesssim t^{\frac{d(d-1)}{2}}$. Since $|X_t| \asymp t^d$ and the induction hypothesis yields $\ell(\gamma_{x,r,t}) \lesssim t^{\frac{(d-1)(d-2)}{2}}\sin r$, the total length of γ_t^r is

$$\ell(\gamma_t^r) = \ell(\gamma_{x,r,t})|X_t| \asymp \sin r\, t^{\frac{(d-1)(d-2)}{2}} t^d \asymp t^{\frac{d(d-1)}{2}+1}\sin r\,. \tag{46}$$

This estimate suggests that we choose $r = r_t$ as $r_t \asymp t^{-1}$. Precisely, let ρ_t be the covering radius of X_t; then we set

$$r_t := 2\rho_t.$$

Therefore, $\sin r \asymp \rho_t \lesssim t^{-1}$, so that (46) leads to the expected total length

$$\ell(\gamma_t^{2\rho_t}) \lesssim t^{-1}t^{\frac{d(d-1)}{2}+1} \asymp t^{\frac{d(d-1)}{2}}.$$

To ensure that $\Gamma_t^{2\rho_t}$ is connected, we will construct $\gamma_{x,2\rho_t,t}$, for $x \in X_t$, in a sequential fashion.

Proof of Theorem 6.1 (Part II). As in Section 5, we consider the graph $\mathcal{G}_{\rho_t}$ with vertices X_t and edges between distinct $x, y \in X_t$ if and only if $B_{\rho_t}(x) \cap B_{\rho_t}(y) \neq \emptyset$. According to Lemma 4.1, the graph $\mathcal{G}_{\rho_t}$ is

https://doi.org/10.1017/fms.2023.106 Published online by Cambridge University Press

connected. Therefore, it possesses a spanning tree $\mathcal{T}_{\rho_t}$ [12]; this is a subgraph that contains all vertices of $\mathcal{G}_{\rho_t}$ such that every vertex y can be reached by a unique path from a root x_0.

We start at the root x_0 of $\mathcal{T}_{\rho_t}$ and take a t-design curve $\gamma_{x_0,2\rho_t,t}$ for $\partial B_{2\rho}(x_0)$. Recall from Lemma 6.5 that $\gamma_{x_0,2\rho_t,t}$ is obtained as the image of a t-design curve γ in $\mathbb{S}^{d-1}$ via the diffeomorphism $\phi_{x_0,2\rho_t}$ as $\gamma_{x_0,2\rho_t,t} = \phi_{x_0,2\rho_t}(\gamma)$ and we suppose that the trajectory of γ is a union of circles.

Now consider the first descendant x_1 of x_0 in the tree $\mathcal{T}_{\rho_t}$. Since $\operatorname{dist}(x_0, x_1) \le 2\rho_t$, Lemma 6.4(ii) (with $r = 2\rho_t$) implies that

$$\partial B_{2\rho_t}(x_0) \cap \partial B_{2\rho_t}(x_1) = \phi_{x_0,2\rho_t}\big(\partial B_\sigma(e_d)\big)$$

for some $\sigma > \pi/4$. Since γ is a t-design curve in $\mathbb{S}^{d-1}$, the covering radius of its trajectory is of the order t^{-1} and is thus smaller than σ for t large enough. Lemma 6.6 implies that $\Gamma \cap \partial B_\sigma(e_d) \neq \emptyset$, and after applying $\phi_{x_0,2\rho_t}$ we obtain that

$$\Gamma_{x_0,2\rho_t,t} \cap \partial B_{2\rho_t}(x_0) \cap \partial B_{2\rho_t}(x_1) \neq \emptyset\,.$$

Let $w_1 \in \mathbb{S}^d$ be a point in this intersection. By Lemma 6.5(iv) applied to $\Psi = \Gamma_{x_0,2\rho_t,t}$ and w_1, there exists a t-design curve $\tilde{\gamma}$ in $\mathbb{S}^{d-1}$, whose image $\phi_{x_1,2\rho_t}(\tilde{\gamma}) = \gamma_{x_1,2\rho_t,t}$ is a t-design for $\partial B_{2\rho}(x_1)$ such that $w_1 \in \Gamma_{x_1,2\rho_t,t}$ and the intersection $\Gamma_{x_0,2\rho_t,t} \cap \Gamma_{x_1,2\rho_t,t}$ contains only finitely many points.

The next descendant x_2 leads to

$$\partial B_{2\rho_t}(x_1) \cap \partial B_{2\rho_t}(x_2) = \phi_{x_1,2\rho_t}\big(\partial B_\sigma(e_d)\big)$$

for some $\sigma > \pi/4$. The same arguments as above yield the existence of

$$w_2 \in \Gamma_{x_1,2\rho_t,t} \cap \partial B_{2\rho_t}(x_1) \cap \partial B_{2\rho_t}(x_2)\,.$$

We now apply Lemma 6.5(iv) with w_2 and $\Psi = \Gamma_{x_0,2\rho_t,t} \cup \Gamma_{x_1,2\rho_t,t}$ and obtain a t-design curve $\Gamma_{x_2,2\rho_t,t}$ in $\partial B_{\rho_t}(x_2)$, such that $w_2 \in \Gamma_{x_2,2\rho_t,t}$ and $\Gamma_{x_2,2\rho_t,t} \cap \big(\Gamma_{x_0,2\rho_t,t} \cup \Gamma_{x_1,2\rho_t,t}\big)$ is finite.

This process is repeated until we reach a leaf of the spanning tree $\mathcal{T}_{\rho_t}$. Then we return to the last branch-off in $\mathcal{T}_{\rho_t}$ and proceed with the next branch of the tree.

Finally, this construction leads to a connected set of circles in $\mathbb{S}^d$, and the resulting trajectory $\Gamma_t := \bigcup_{x \in X_t} \Gamma_{x,2\rho_t,t}$ of all curves is a connected set with finitely many intersection points.

By construction, Γ_t is a connected set of finitely many circles. Although Lemma 5.2 is formulated for a graph $\mathcal{G}$ constructed from finitely many circles in $\mathbb{S}^2$, its proof only uses combinatorial arguments and hence also holds for circles in $\mathbb{S}^d$. Since Γ_t is connected, so is $\mathcal{G}$. The second part of the proof of Lemma 5.2 shows that we may fix an arbitrary orientation, and then the corresponding directed graph $\mathcal{G}_{\rightarrow}$ is also connected. Thus, Γ_t can be traversed by a single continuous curve. See again Figure 3 for a pictorial argument. □

7. Some applications

We now discuss a few direct applications of t-design curves to mobile sampling on the sphere and exact integration of polynomials with respect to the measure $\mathrm{e}^{-\|x\|}\mathrm{d}x$ on $\mathbb{R}^d$.

7.1. Mobile sampling on the sphere

Here we prove Corollary 1.4 of the Introduction and show that a polynomial f of degree t can be reconstructed from its restriction to a $2t$-design curve.

For its formulation, we recall that Π_t restricted to $\mathbb{S}^d$ is a reproducing kernel Hilbert space with respect to the inner product from $L^2(\mathbb{S}^d)$. This means that for every $x \in \mathbb{S}^d$, there is a polynomial $k_x \in \Pi_t$, such that

https://doi.org/10.1017/fms.2023.106 Published online by Cambridge University Press

$$f(x) = \langle f, k_x \rangle = \int_{\mathbb{S}^d} f\, \overline{k_x}\,.$$

This kernel possesses an explicit description by means of zonal spherical harmonics and Gegenbauer (or ultraspherical) polynomials [43]. Let P_k^λ, $k \in \mathbb{N}$, be the sequence of Gegenbauer polynomials associated with $\lambda > 0$. They are defined by their generating function

$$(1 - 2rx + r^2)^{-\lambda} = \sum_{k=0}^{\infty} P_k^\lambda(x) r^k\,.$$

Using [43, Thm. 2.14], there are real constants $b_{k,d}$, such that

$$k_x(y) = \sum_{k=0}^{t} b_{k,d} P_k^{\frac{d-1}{2}}(x \cdot y) \qquad x, y \in \mathbb{S}^d\,. \tag{47}$$

We can now extend the formulation of Corollary 1.4 of the Introduction as follows.

Proposition 7.1. *Let γ be a $2t$-design curve on $\mathbb{S}^d$ and f a restriction of a polynomial of degree t onto $\mathbb{S}^d$. Then*

$$\frac{1}{\ell(\gamma)} \int_\gamma |f|^2 = \int_{\mathbb{S}^d} |f|^2, \tag{48}$$

and f is reconstructed from its values along γ by

$$f(x) = \frac{1}{\ell(\gamma)} \int_\gamma f k_x, \quad \text{for all } x \in \mathbb{S}^d\,. \tag{49}$$

Proof. We only need to prove the reconstruction formula (49). Since $f k_x \in \Pi_{2t}$ and k_x is real-valued, the reproducing property yields

$$f(x) = \int_{\mathbb{S}^d} f\, k_x = \frac{1}{\ell(\gamma)} \int_\gamma f k_x\,. \qquad \square$$

7.2. *Integration of polynomials on $\mathbb{R}^d$ with respect to $\mathrm{e}^{-\|x\|}\mathrm{d}x$*

Next we consider the integration problem

$$\int_{\mathbb{R}^d} f(x) \mathrm{e}^{-\|x\|} \mathrm{d}x.$$

Recall that the family of generalized Laguerre polynomials $(L_n^{(d-1)})_{n\in\mathbb{N}}$ are orthogonal with respect to the measure $r^{d-1}\mathrm{e}^{-r}\mathrm{d}r$ on $[0,\infty)$. Using the zeros of $L_n^{(d-1)}$, we obtain the following quadrature rule, where Π_t now stands for polynomials of degree at most t in d variables.

Corollary 7.2. *Let γ be a spherical t-design curve in $\mathbb{S}^{d-1}$. For every integer $n \geq \frac{t+1}{2}$, let $\{r_j\}_{j=1}^n \subset (0,\infty)$ be the set of zeros of $L_n^{(d-1)}$ with the associated weights $\{w_j\}_{j=1}^n \subset (0,\infty)$ for Gaussian quadrature. Then we have*

$$\int_{\mathbb{R}^d} f(x) \mathrm{e}^{-\|x\|} \mathrm{d}x = \frac{\mathrm{vol}(\mathbb{S}^{d-1})}{\ell(\gamma)} \sum_{j=1}^{n} \frac{w_j}{r_j} \int_{r_j\gamma} f, \qquad \text{for all } f \in \Pi_t.$$

Thus, the scaled curves $\{r_j\gamma\}_{j=1}^n$ with weights $\{\frac{w_j\,\mathrm{vol}(\mathbb{S}^{d-1})}{r_j \ell(\gamma)}\}_{j=1}^n$ form an exact quadrature rule for Π_t with respect to the measure $\mathrm{e}^{-\|x\|}\mathrm{d}x$.

https://doi.org/10.1017/fms.2023.106 Published online by Cambridge University Press

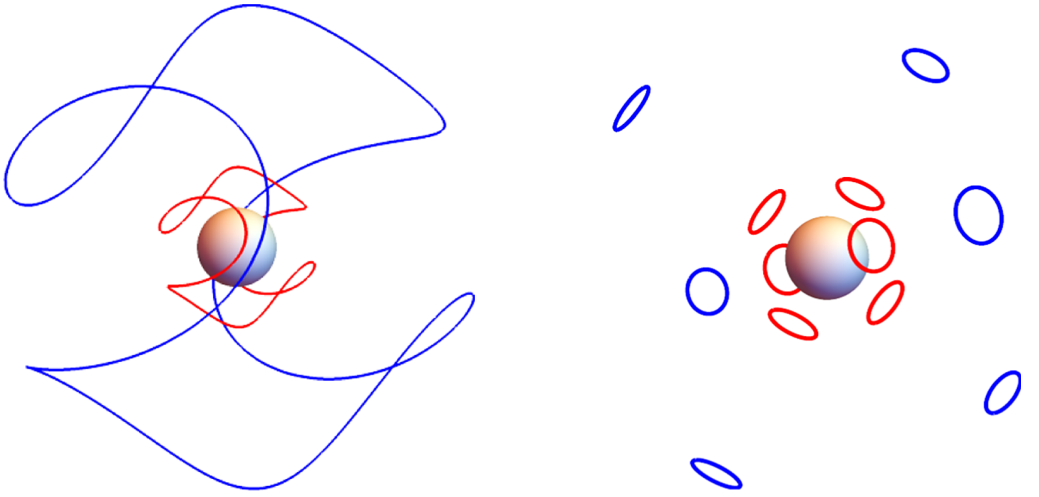

(a) The trajectories (red) $2\Gamma^{(3,\alpha_3)}$ and (blue) $6\Gamma^{(3,\alpha_3)}$ in Example 7.3.

(b) Circles centered at 3-design points in spheres of radius 2 and 6.

Figure 4. *Trajectories provide exact integration of all polynomials in three variables of degree at most* 3 *with respect to the measure* $\mathrm{e}^{-\|x\|}\mathrm{d}x$. *The unit sphere in the center is shown as a reference.*

Proof. Gaussian quadrature based on the zeros of $L_n^{(d-1)}$ is exact for all univariate polynomials g of degree at most $t \le 2n-1$; that is,

$$\int_0^\infty g(r) r^{d-1} \mathrm{e}^{-r} \mathrm{d}r = \sum_{j=1}^n w_j g(r_j).$$

Let $f \in \Pi_t$. For fixed $z \in \mathbb{S}^{d-1}$, the function $r \mapsto f(rz)$ is a univariate polynomial of degree at most t, and therefore,

$$\begin{aligned}\int_{\mathbb{R}^d} f(x)\mathrm{e}^{-\|x\|}\mathrm{d}x &= \int_{\mathbb{S}^{d-1}} \int_0^\infty f(rz) r^{d-1} \mathrm{e}^{-r} \mathrm{d}r \mathrm{d}z \\ &= \int_{\mathbb{S}^{d-1}} \Big(\sum_{j=1}^n w_j f(r_j z) \Big) \mathrm{d}z.\end{aligned}$$

Since γ is a t-design curve on $\mathbb{S}^{d-1}$ and $z \mapsto f(r_j z)$ is a polynomial in Π_t, we derive

$$\begin{aligned}\int_{\mathbb{R}^d} f(x)\mathrm{e}^{-\|x\|}\mathrm{d}x &= \frac{\mathrm{vol}(\mathbb{S}^{d-1})}{\ell(\gamma)} \int_\gamma \sum_{j=1}^n w_j f(r_j \cdot) \\ &= \frac{\mathrm{vol}(\mathbb{S}^{d-1})}{\ell(\gamma)} \sum_{j=1}^n w_j \int_0^1 f(r_j \gamma(s)) \|\dot\gamma(s)\| \mathrm{d}s \\ &= \frac{\mathrm{vol}(\mathbb{S}^{d-1})}{\ell(\gamma)} \sum_{j=1}^n \frac{w_j}{r_j} \int_0^1 f(r_j \gamma(s)) \|r_j \dot\gamma(s)\| \mathrm{d}s \\ &= \frac{\mathrm{vol}(\mathbb{S}^{d-1})}{\ell(\gamma)} \sum_{j=1}^n \frac{w_j}{r_j} \int_{r_j\gamma} f.\end{aligned}$$

□

https://doi.org/10.1017/fms.2023.106 Published online by Cambridge University Press

Example 7.3. Let $\gamma^{(3,a_3)}$ be the spherical 3-design curve of Proposition 3.1. The zeros of $L_2^{(2)}(r) = \frac{1}{2}r^2 - 4r + 6$ are $r_1 = 2$ and $r_2 = 6$. The associated Gaussian weights are $w_1 = \frac{3}{2}$ and $w_2 = \frac{1}{2}$. Therefore, we obtain

$$\int_{\mathbb{R}^3} f(x)\mathrm{e}^{-\|x\|}\mathrm{d}x = \frac{3\pi}{\ell(\gamma^{(3,a_3)})}\int_{2\gamma^{(3,a_3)}} f + \frac{\pi}{3\ell(\gamma^{(3,a_3)})}\int_{6\gamma^{(3,a_3)}} f, \tag{50}$$

for $f \in \Pi_3$; see (a) in Figure 4.

Example 7.4. Consider t-design points $X_t \subset \mathbb{S}^2$ and take curves $\gamma_{x,r}$ whose trajectory are Euclidean circles $\Gamma_{x,r}$ of radius $\sin r$ centered at $x \in X_t$ as in the proof of Theorem 5.1. Analogous to Corollary 7.2, we may scale via the zeros of $L_n^{(d-1)}$ and use the associated Gaussian quadrature weights to obtain

$$\int_{\mathbb{R}^3} f(x)\mathrm{e}^{-\|x\|}\mathrm{d}x = \frac{2}{\sin r|X_t|}\sum_{j=1}^{n}\sum_{x\in X_t}\frac{w_j}{r_j}\int_{r_j\gamma_{x,r}} f, \qquad f \in \Pi_t;$$

see (b) in Figure 4 for $t = 3$.

Funding statement. K. G. was supported in part by the project P31887-N32 of the Austrian Science Fund (FWF).

Competing interest. The authors have no competing interest to declare.

References

[1] A. Barg, 'Bounds on packings of spheres in the Grassmann manifold', *IEEE Trans. Inform. Theory* **48**(9) (2002), 2450–2454.
[2] J. J. Benedetto and H.-C. Wu, 'Non-uniform sampling and spiral MRI reconstruction', in *Wavelet Applications in Signal and Image Processing VIII* vol. 4119 (International Society for Optics and Photonics, 2000), 130–142.
[3] A. Bondarenko, D. Radchenko and M. Viazovska, 'Optimal asymptotic bounds for spherical designs', *Ann. Math.* **178**(2) (2013), 443–452.
[4] L. Brandolini, C. Choirat, L. Colzani, G. Gigante, R. Seri and G. Travaglini, 'Quadrature rules and distribution of points on manifolds', *Ann. Sc. Norm. Super. Pisa Cl. Sci.* **13**(4) (2014), 889–923.
[5] J. S. Brauchart, E. B. Saff, I. H. Sloan and R. S. Womersley, 'QMC designs: Optimal order quasi Monte Carlo integration schemes on the sphere', *Math. Comp.* **83** (2014), 2821–2851.
[6] A. Breger, M. Ehler and M. Gräf, 'Points on manifolds with asymptotically optimal covering radius', *J. Complexity* **48** (2018), 1–14.
[7] J. Cantarella, R. B. Kusner and J. M. Sullivan., 'On the minimum ropelength of knots and links', *Invent. Math.* **150** (2002), 257–286.
[8] J. Chen, L. Yu and W. Wang, 'Hilbert space filling curve based scan-order for point cloud attribute compression', *IEEE Trans. Image Process.* **31** (2022), 4609–4621.
[9] P. de la Harpe and C. Pache, 'Cubature formulas, geometrical designs, reproducing kernels, and Markov operators', *in Infinite Groups: Geometric, Combinatorial and Dynamical Aspects* vol. 248 (Birkhäuser, Basel, 2005), 219–267.
[10] P. Delsarte, J. M. Goethals and J. J. Seidel, 'Spherical codes and designs', *Geom. Dedicata* **6** (1977), 363–388.
[11] J. Dick, M. Ehler, M. Gräf and C. Krattenthaler, 'Spectral decomposition of discrepancy kernels on the Euclidean ball, the special orthogonal group, and the Grassmannian manifold', *Constr. Approx.* **57**(3) (2023), 983–1026.
[12] R. Diestel, *Graph Theory* (Graduate Texts in Mathematics), fifth edn. (Springer, Berlin, 2018). Paperback edition of [MR3644391].
[13] M. Ehler, U. Etayo, B. Gariboldi, G. Gigante and T. Peter, 'Asymptotically optimal cubature formulas on manifolds for prefixed weights', *J. Approx. Theory* **271**(105632) (2021).
[14] M. Ehler, M. Gräf, S. Neumayer and G. Steidl, 'Curve based approximation of measures on manifolds by discrepancy minimization', *Found. Comput. Math.* **21**(6) (2021), 1595–1642.
[15] U. Etayo, J. Marzo and J. Ortega-Cerdà, 'Asymptotically optimal designs on compact algebraic manifolds', *Monatsh. Math.* **186**(2) (2018), 235–248.
[16] B. Gariboldi and G. Gigante, 'Optimal asymptotic bounds for designs on manifolds', *Anal. PDE* **14** (2021), 1701–1724.
[17] H. Gerlach and H. von der Mosel, 'On sphere-filling ropes', *Amer. Math. Monthly* **118**(10) (2011), 863–876.
[18] H. Gerlach and H. von der Mosel, 'What are the longest ropes on the unit sphere', *Arch. Ration. Mech. Anal.* **201** (2011), 303–342.
[19] M. Ghomi and J. Wenk, 'Shortest closed curve to inspect a sphere', *J. Reine Angew. Math.* 2021(781) (**2021**), 57–84.
[20] B. Goertzel, 'Global optimization with space-filling curves', *Appl. Math. Lett.* **12** (1999), 133–135.

https://doi.org/10.1017/fms.2023.106 Published online by Cambridge University Press

[21] M. Gräf and D. Potts, 'On the computation of spherical designs by a new optimization approach based on fast spherical Fourier transforms', *Numer. Math.* **119** (2011), 699–724.
[22] K. Gröchenig, J. L. Romero, J. Unnikrishnan and M. Vetterli, 'On minimal trajectories for mobile sampling of bandlimited fields', *Appl. Comput. Harmon. Anal.* **39**(3) (2015), 487–510.
[23] T. Hastie and W. Stuetzle, 'Principal curves', *J. Amer. Statist. Assoc.* **84**(406) (1989), 502–512.
[24] S. Hauberg, 'Principal curves on Riemannian manifolds', *IEEE Trans. Pattern Anal. Mach. Intell.* **38**(9) (2015), 1915–1921.
[25] P. Jaming, F. Negreira and J. L. Romero, 'The Nyquist sampling rate for spiraling curves', *Appl. Comput. Harmon. Anal.* **52** (2021), 198–230.
[26] B. Jaye and M. Mitkovski, 'A sufficient condition for mobile sampling in terms of surface density', *Appl. Comput. Harmon. Anal.* **61** (2022), 57–74.
[27] K. Kang, R. M. Shapley and H. Sompolinsky, 'Information tuning of populations of neurons in primary visual cortex', *J. Neurosci.* **24**(15) (2004), 3726–3735.
[28] B. Kegl, A. Krzyzak, T. Linder and K. Zeger, 'Learning and design of principal curves', *IEEE Trans. Pattern Anal. Mach. Intell.* **22**(3) (2000), 281–297.
[29] J. Korevaar and J. L. H. Meyers, 'Spherical Faraday cage for the case of equal point charges and Chebyshev-type quadrature on the sphere', *Integral Transforms Spec. Funct.* **1**(2) (1993), 105–117.
[30] S. M. LaValle, *Planning Algorithms* (Cambridge Univ. Press, Cambridge, 2006).
[31] J. Lee, J.-H. Kim and H.-S. Oh, 'Spherical principal curves', *IEEE Trans. Pattern Anal. Mach. Intell.* **43**(6) (2021), 2165–2171.
[32] C. Müller, *Spherical Harmonics* vol. 17 (Springer-Verlag, 1966).
[33] J. O'Hara, 'Family of energy functionals of knots', *Topology Appl.* **48** (1992), 147–161.
[34] C. P. Oliveira and J. Buescu, 'Mixed integral identities involving unit spheres and balls in complex context', *Internat. J. Math.* **26**(14) (2015), 1550115.
[35] S. Ramamoorthy, R. Rajagopal and L. Wenzel, 'Efficient, incremental coverage of space with a continuous curve', *Robotica* **26** (2008), 503–512.
[36] A. Rashkovskii, A. Ulanovskii and I. Zlotnikov, 'On 2-dimensional mobile sampling', *Appl. Comput. Harmon. Anal.* **62** (2023), 1–23.
[37] D. L. Ringach, 'Population coding under normalization', *Vision Research* **50** (2010), 2223–2232.
[38] W. Rudin, *Real and Complex Analysis*, third edn. (McGraw-Hill Book Co., New York, 1987).
[39] S. G. Samko, 'Generalized Riesz potentials and hypersingular integrals with homogeneous characteristics, their symbols and inversion', *Proc. Steklov Inst. Math.* **2** (1983), 173–243.
[40] J. J. Seidel, 'Definitions for spherical designs', *J. Statist. Plann. Inference* **95**(1–2) (2001), 307–313.
[41] P. Seymour and T. Zaslavsky, 'Averaging sets: a generalization of mean values and spherical designs', *Adv. Math.* **52** (1984), 213–240.
[42] I. H. Sloan and R. S. Womersley, 'Extremal systems of points and numerical integration on the sphere', *Adv. Comput. Math.* **21** (2004), 107–125.
[43] E. Stein and G. Weiss, *Introduction to Fourier Analysis on Euclidean Spaces* (Princeton University Press, Princeton, N.J., 1971).
[44] P. Tsinganos, B. Cornelis, J. Cornelis, B. Jansen and A. Skodras, 'Hilbert sEMG data scanning for hand gesture recognition based on deep learning', *Neural Comput. & Applications* **33** (2021), 2645–2666.
[45] J. Unnikrishnan and M. Vetterli, 'Sampling and reconstruction of spatial fields using mobile sensors', *IEEE Trans. Signal Process.* **61**(9) (2013), 2328–2340.
[46] J. Unnikrishnan and M. Vetterli, 'Sampling high-dimensional bandlimited fields on low-dimensional manifolds', *IEEE Trans. Inform. Theory* **59**(4) (2013), 2103–2127.
[47] R. J. Wilson, *Introduction to Graph Theory* (Addison Wesley, Longman Limited, 1998).
[48] R. S. Womersley, 'Efficient spherical designs with good geometric properties', in J. Dick, F. Kuo and H. Wozniakowski, eds., *Contemporary Computational Mathematics - A Celebration of the 80th Birthday of Ian Sloan* (Springer, 2018), 1243–1285.
[49] C. Yu, H. Schumacher and K. Crane, 'Repulsive curves', *ACM Trans. Graph.* **40**(2) (2021).
[50] V. A. Zalgaller, 'Shortest inspection curves for the sphere', *J. Math. Sci.* **131** (2005), 5307–5320.

https://doi.org/10.1017/fms.2023.106 Published online by Cambridge University Press